Tampereen ammattikorkeakoulu

Temperature Dependence of Surface Free Energy on Polymers

Rauno Myllynen

Bachelor's Thesis
May 2019

Degree Programme in Laboratory Engineering

TIIVISTELMÄ

Tampereen ammattikorkeakoulu
Laboratoriotekniikan koulutus

MYLLYNEN, RAUNO:
Polymeerien pintaenergian lämpötilariippuvuus

Opinnäytetyö 68 sivua, joista liitteitä 5 sivua
Toukokuu 2019

Jään ja biomateriaalin kertyminen erilaisille pinnoille aiheuttaa vuosittain mittaamattomat taloudelliset menetykset ilmailuliikenteelle, merenkululle ja energian siirrolle. Näiden ongelmien ratkaisemiseksi tehdään valtavasti tutkimusta, jossa Tampereen teknillisen yliopiston materiaalitekniikan laboratorio on osallisena. Laboratoriossa kehitetään pintaratkaisuja, jotka pinnan mikrorakenteen ja matalan pintaenergian ansiosta estävät arktisissa olosuhteissa jään muodostumista. Tässä oletuksena on jään käyttäytyvän saman tapaisesti pinnalla kuin veden, mutta ei ole ollut olemassa julkaistua tietoa, onko pintaenergialla riippuvaisuutta mittauslämpötilaan.

Tämän opinnäytetyön tavoitteena oli kehittää menetelmä polymeeristen kiinteiden näytteiden pintaenergian määrittämiseen matalissa lämpötiloissa. Tämän opinnäytetyön tarkoitus oli määrittää viiden polymeerimateriaalin (PE, UHMW-PE, PP, PTFE ja PU) pintaenergia muuttuvissa lämpötiloissa kontaktikulma-analysaattorilla käyttäen Peltier plate -tekniikkaa tutkittavien näytteiden lämpötilan säätämiseen ja täten pintaenergian mahdollinen lämpötilakorrelaatio.

Työssä määritettiin tutkittavien polymeerinäytteiden kontaktikulmaa veden, etyleeniglykolin ja dijodometaanin kanssa Peltier plate -tekniikalla huoneenlämmössä, +15 °C, +10 °C sekä +5 °C lämpötiloissa. Näistä mittaustuloksista laskettiin OWRK-menetelmällä näytemateriaaleille pintaenergiat kussakin lämpötilassa ja laadittiin kuvaajat mittauslämpötilan vaikutuksesta.

Työn tuloksena havaittiin trendi, jonka mukaisesti mittausnesteiden kontaktikulmat näytteiden kanssa pienenivät mittauslämpötilan madaltuessa. Tämä aiheuttaa pintaenergian kasvun näytteille lämpötilan laskiessa, mutta mittaustulosten pohjalta ei matemaattista kaavaa muutokselle voida vielä laatia.

Tutkimuksen jatkamiseksi täytyy mittausolosuhteita kehittää ilmankosteuden osalta, sillä tämä aiheutti ongelmia matalissa lämpötiloissa. Erityisesti tämä korostui, kun haluttiin näytteistä useampi mittaustulos samassa lämpötilassa, Tämä osoittautui pulmalliseksi Peltier platen pienen näytepöydän kanssa toimittaessa, sillä tämä mahdollisti vain kolmen pisaran mittaamisen, ennen kuin näytekammio piti avata ja näyte puhdistaa ennen uudelleen asettelua pöydälle. Myöskin näytteet tulee jatkossa laatia paremmin työhön sopivaksi, sillä 6-8 mm paksujen näytteiden lämpötilan muutos vei suuren osan mittausajasta.

Asiasanat: pintaenergia, polymeeri, kontaktikulma, lämpötila

ABSTRACT

Tampereen ammattikorkeakoulu
Tampere University of Applied Sciences
Degree Programme in Laboratory Engineering

MYLLYNEN, RAUNO:
Temperature Dependence of Surface Free Energy on Polymers

Bachelor's thesis 68 pages, appendices 5 pages
May 2019

Biofouling and heavy accretion of ice is known to cause massive financial losses to aviation, maritime logistics and energy transportation every year. The Laboratory of Material Science at Tampere University of Technology is involved in international research to tackle these problems. Among the subjects studied in the laboratory are surface coatings and structures which prevent accretion of ice, due to the micro structure of the surface and low surface free energy. It was hypothesised that accretion of ice is closely related to wetting of the surface, but no prior research existed whether there is correlation between surface free energy and ambient temperature.

The purpose of this thesis was to develop a method for determination of surface free energy from solid polymer samples in low temperatures. The goal of the thesis was to determine surface free energy of five different polymer materials (PE, UHMW-PE, PP, PTFE and PU) in different temperatures. The measurements were made by Krüss 100S Drop shape analysis system using Peltier plate technique to adjust temperature of samples and thus find if there is correlation between temperature and surface free energy.

According to the results of this research there was a trend of decreasing contact angle when temperature was lowered. Because of this, surface free energy increases when temperature is lowered. However, the measurement results were inadequate for calculating mathematical formula to describe this phenomenon.

For future research, the measurement conditions need to be adjusted. Especially humidity in the environmental chamber caused numerous problems in lower temperatures when multiple sample droplets were deposited on the sample. This caused humidity related problems as the measurement table of Peltier plate allows only three droplets per sample before it must to be cleaned and repositioned. Also, in the future samples need to be better designed and prepared for Peltier plate as it took a major portion of measurement time to cool polymer samples which were 6 to 8 millimetres thick.

Key words: surface free energy, polymer, contact angle, temperature, peltier plate

SISÄLLYS

ABBREVIATIONS

CA	Contact angle
DIM	Diiodomethane
EtGl	Ethylene Glycol (in result table)
HDPE	High density polyethylene
LDPE	Low density polyethylene
OWRK	Owens-Wendt-Rabel and Kaelble
PDMS	Polydimethylsiloxane
PE	Polyethylene
PE-UHMW	Ultra high molecular weight polyethylene
PP	Polypropylene
PTFE	Polytetrafuoroethylene
PU	Polyurethane
SLIPS	Slippery liquid infused porous surface
SFE	Surface free energy

1 INTRODUCTION

This bachelor's thesis was done for Laboratory of Material Science, Tampere University of Technology. Materials which are used as well in high as in low temperatures are studied and developed in the laboratory. The thesis was background research for slippery liquid-infused porous surfaces for anti-icing applications (SLIPS) project as part of international anti-icing research. The aim of anti-icing research is to find surface coatings which prevent accretion of ice and biofouling in arctic environment. The hypothesis of this thesis was that there exists a correlation between surface free energy and temperature.

The purpose of this thesis was to develop a method for determination of surface free energy from solid polymer samples in low temperatures. During the research there was no documented research if there is correlation between temperature and surface free energy.

The goal of the thesis was to determine surface free energy of five different polymer materials (PE, UHMW-PE, PP, PTFE and PU) in different temperatures. The measurements were made by Krüss 100S Drop shape analysis system using Peltier plate- technique to adjust temperature of samples and thus find if there is correlation between surface free energy and temperature.

2 POLYMERS

The word polymer is derived from Greek words poly, meaning many, and mere meaning part. Simply stated, polymer is a long-chain molecule that is composed of large number of repeating units of identical structure.

Polymers that are used by industry are also called as plastics. Plastic can be defined as follows: plastics are solid macromolecular polymers that are produced by chemical industry or mixtures that contain substantive portion of them. Common feature to plastics is that they are moulded during manufacture process usually by heat and pressure. Only few polymers can be used as such for manufacturing plastic products. It is often mixed additives to polymers for enhance plasticity, physical and chemical durability. (Seppälä, 1999, 1)

A world without plastics, or synthetic organic polymers, seems nowadays unimaginable, yet the large-scale production and use only dates back to 1950's. Although the first synthetic plastics appeared in early 20th century, widespread use outside military did not occur until after World War II. Largest groups on nonfibrous plastics production are polyethylene (36%), polypropylene (22%), polyvinylchloride (12%), followed by polyethylene terephthalate, polyurethane and polystyrene (<10% each). (Geyer, 2017,1)

2.1 Classification of polymers and plastics

Polymers can be divided into groups by their origin, structure, properties and use. It is also used classification by their crystallinity, polymerisation mechanism and reactions.

2.1.1 Classification by origin

By origin polymers are divided into three different groups. Natural polymers or biopolymers synthesised by organisms and essential for our existence. Humans first relied on natural polymers for clothing, wrapping ourselves in animal skins and furs. Polymers found in nature such as cellulose, starch, proteins, natural rubber, gutta-percha, lignin, resins and DNA. (Bruice, 2001,1105)

Semisynthetic polymers are prepared from natural polymers by chemical treatment. Due this they are also called modified natural polymers. Examples of semisynthetic polymers are cellulose nitrate, cellulose acetate, vulcanised rubber and ebonite.

Synthetic polymers are manufactured by chemical industry from small molecule raw materials called monomers. In polymerisation process monomers are linked together forming macromolecule. Nowadays mostly used polymers such as polyethene, polyvinylchloride, polypropylene, polystyrene and polyethylene terephthalate are synthetic polymers.

2.1.2 Classification by structure

When polymer is formed from one source material or monomer, it is called homopolymer. Molecule structure of homopolymer can be linear, branched or bridged. In linear polymer, the monomer units are lined to each other as a chain. In branched homopolymer polymer frame has short branches, that vary from one to hundreds of monomers, connected to the main frame. In bridged homopolymer monomer units are linked to each other forming three-dimensional web structure. (Seppälä, 1999, 8)

Often it is possible to obtain polymers with desirable properties by linking two or three different repeating units during polymerisation. Polymers with two different repeating units in their chain are called copolymers. The less frequent case with three chemically different repeating units, are called terpolymers. Commercially, the most important copolymers are derived from vinyl monomers such as styrene, ethylene, acrylonitrile and vinyl chloride. (Fried, 2003, 10)

2.1.3 Thermoplastics, thermosetting plastics and elastomers

All polymers can be divided into two major groups based on their thermal processing behaviour. Those polymers that can be heat-softened in order to process into desired form are called thermoplastics. Waste thermoplastics can

be recovered and refabricated by application of heat and pressure. Polystyrene is good example of commercial thermoplastic. Polyolefins (e.g. polyethylene and polypropylene) are other major examples. (Fried, 2003, 4)

In comparison, thermosets are polymers whose individual chains have been chemically by covalent bonds during polymerisation or by chemical or thermal treatment during fabrication. Once formed, these crosslinked networks cannot be thermally processed. This property makes thermosets suitable material for coatings and adhesive applications. The most used thermosets are unsaturated polyesters, polyepoxies and polyphenols. (Seppälä, 1999, 11)

Elastomers fall between these two major groups. In elastomer, long polymer chains are chemically linked to each other (e.g. bridging). It is characteristic for elastomers to stretch and then to revert into their original measure and shape after stress. Rubber is the most known elastomer. Natural rubber has linear structure. In rubber sulphur forms bridges between molecules, but the amount of crosslinking is minute compared to thermosets.

Some polymers that have linear or branched structure, behave more like thermoplastics than thermoset. In polytetrafluoroethene (PTFE) this feature is caused by large size of the molecule, rigidity and high crystallinity. In cellulose strong hydrogen bonds between molecules inhibit molecular movement. (Seppälä, 1999, 12)

2.1.4 Classification based upon polymerisation mechanism

In addition to classifying polymers on the basis of their processing characteristics, polymers can also be classified according to the mechanism of polymerisation. Most used approach is to classify polymers either addition or condensation polymers. This classification was developed by Wallace Carothers, a pioneer of the polymer industry at DuPont. (Fried, 2003, 5)

Addition polymers also known as chain-growth polymers, are made by addition of monomers to the end of growing chain. Addition polymerisation process does not produce any small-molecular by-products during process. Thus, the repeating

unit of polymer has the same structure as the monomer used for production. The monomer unit consists at least one double bond allows the polymerisation process to occur. This polymerisation process is carried out by initiator or catalyst in raised temperature and end of polymer chain is reactive because it is either radical, anion or cation.

Condensation polymers, also called as step-growth polymers, are combining two molecules while removing a small molecule, usually water or alcohol, from the structure. The reacting molecules have reactive functional groups at each end. Unlike in addition polymers, which requires individual molecules to add to the end of growing chain, any two reactive molecules can combine in step-growth polymerisation.

2.2 Examples of most common plastics

2.2.1 Polyethylene

Ethylene, one of the most important petrochemicals, may be polymerised by a variety of techniques to produce products as diverse as low-molecular-weight waxes to highly crystalline high-molecular-weight polyethylene (HDPE). The first commercial polyolefin was low-crystallinity, low-density polyethylene (LDPE) produced by ICI in 1939. (Fried, 2003,355)

The structure of polyethylene is linear, but it may contain branches of different length depending on production method. This linear structure makes polyethylene thermoplastic. Commercial polyethylene can be divided into two main groups depending on production method and properties. Low density polyethylene, LDPE, contains short and long branches. LDPE is produced by radical polymerisation in high pressure. High density polyethylene, HDPE, has straight polymer chain. HDPE is produced by catalytic polymerisation in low pressure.

LDPE is produced by free-radical bulk polymerisation using traces of oxygen or peroxide as initiator. Polymerisation is conducted either in high pressure autoclaves or in continuous tubular reactors operating at temperatures near 250

°C and pressures as high as 300 atm. The free-radical polymerisation of ethylene produces highly branched molecule, even though most of the branches are ethylene or butylene.

Due the short branches, crystallinity of LDPE is just 50 - 70% and density is between 0,910 - 0,925 $\frac{g}{cm^3}$. Tensile strength of LDPE falls in between 4 -10 MPa. Molecular weights of LDPE typically fall in the range between 6000 and 50000 u. The majority of LDPE is used as thin film for packaging, while the remaining production finds use in wire and cable insulation, coatings and injection-moulded products. (Fried, 2003, 356)

HDPE is more rigid and firm than LDPE due the higher crystallinity. Production of HDPE became possible with the discovery of catalytic polymerisation of ethylene. Catalytic process changed industrial polymerisation of ethylene, as it made possible to carry out process in lower temperatures and pressure. This discovery of catalytic polymerisation earned Karl Ziegler and Giulio Natta Nobel Prize in Chemistry 1963. (Seppälä, 1999, 131)

HDPE has reduced branching compared to LDPE, which can be obtained by polymerisation ethylene in the presence of coordination catalysts. There are two main catalytic processes for production of HDPE. Firstly, there is the Philips-type process, which consists chromium oxide, CrO_3, supported on aluminium oxide or silica-alumina. Polymerisation is conducted at 100 atm and 200 °C in hydrocarbon solvents in which catalysts are insoluble.

Secondly, there is Ziegler or Ziegler-Natta catalysts, which are typically complexes of aluminium trialkyls and titanium or other transition-metal halides. This process can be conducted at 1 - 10 atm and 60 - 75 °C to obtain high molecular weight linear polymers. With this method molecular weight is 10000 – 100000 u with much narrower weight distribution than Philips-type polymers or LDPE.

Due the low branching, crystallinity of HDPE is 80 - 95% and density is between 0,94 - 0,97 $\frac{g}{cm^3}$ depending on polymerisation process. Also, the tensile strength

of HDPE is higher than LDPE, between 20 - 35 MPa. The principal commercial applications for HDPE include blow-molded containers, crates, drums and gas tanks.

Using low pressure process it is possible to manufacture polyethylene having molecular weight in the range of 1 to 5 million. This polyethylene is called ultra-high molecular weight PE or UHMWPE. UHMWPE is chemically inert, it has exceptional impact and tensile strength, tear and puncture resistance, low coefficient of friction and good fatigue resistance. Applications of UHMWPE include orthopaedic implants such as artificial hip replacements, battery separators, grocery sacks and as additive to improve the sliding and wear behaviour of other thermoplastics. (Fried, 2003, 414)

2.2.2 Polypropylene

Polypropylene (PP) is lightweight plastic with moderately high melting temperature, which is used to manufacture pipes, sheet, blow-molded containers and textile fibres. Almost all the commercial polypropylene is isotactic, i.e. all methylene substituents are on same side of macromolecular backbone. This enables high crystallinity and thus high tensile strength as well as melting temperature. Like polyethylene, polypropylene is also thermoplastic. (Seppälä, 1999, 140)

The first commercial plastic, introduced in 1957, was highly isotactic. The polymerisation process had great resemblance to Ziegler-Natta process of polyethylene. High-molecular-weight isotactic PP can be obtained by using heterogenous catalyst of a violet crystalline titanium chloride with cocatalyst, usually an organoaluminium compound such as diethyl aluminium chloride. Catalysts are slurred in a hydrocarbon mixture, which helps heat transfer in batch or continuous reactors operating at temperatures of 50 -80 °C and pressure of 5 to 25 atm. (Fried, 2003, 358)

At room temperature PP is not soluble in any solvents but softens at +60 °C in xylene, aromatic and chlorinated hydrocarbons. Due the tertiary carbon atoms

PP is less susceptible to UV radiation and oxygen and thus it always needs to add stabilizer.

2.2.3 Polytetrafluoroethylene

Fluorocarbon polymers are a specialty amongst polymers as those are capable of meeting demanding service applications, including operation over broad temperature range, exposure to wide range of chemicals and petroleum products. Due to high price fluoropolymers they have limited commercial usage.

Among the most important fluoropolymers is polytetrafluoroethylene (PTFE), also known as Teflon™, obtained by the emulsion free-radical polymerisation of tetrafluoroethylene. Teflon™ was discovered accidentally by Roy J. Plunket and Jack Rebok who were working on new refrigerants as DuPont in 1938. Plunket and Rebok noticed that tetrafluoroethylene gas stored in high-pressure vessel in dry ice solidified into a smooth, waxy white powder. This powder seemed impervious to liquids and could not be melted under ordinary conditions. (Fried, 2003, 403)

Commercially produced PTFE is highly dense, about 2,2 $\frac{\mathrm{g}}{\mathrm{cm}^3}$ with stability in high temperatures, low-temperature flexibility chemically inert and it has extremely low coefficient of friction. Limited processability of PTFE is attributed to high crystallinity and high crystalline-melting temperature, 327 °C. These are resulting from highly regular structure and high molecular weight, 400 000 – 9 000 000 u. PTFE is used to manufacture pipes, discs, bars, films and fibres. (Seppälä, 1999, 153)

2.2.4 Polyurethane

Polyurethanes (PU) were developed by O. Beyer at I.G. Farbenindustrie in 1937, but it was not until 1950’s when commercial production initiated. These polymers have high strength, high abrasion resistance, good resistance to gases, oil and aromatic hydrocarbons and excellent resistance to oxygen. Depending on quality and amount of starting materials, and additives, the resulting polymer is thermoplastic, thermoset or elastomer. (Seppälä, 1999, 123)

There are generally two major pathways for preparing polyurethanes. It can be prepared either by step-growth polymerisation of diisocyanate with diol compounds or by the reaction of bischloroformate with diamine. These routes are illustrated in figure 1.

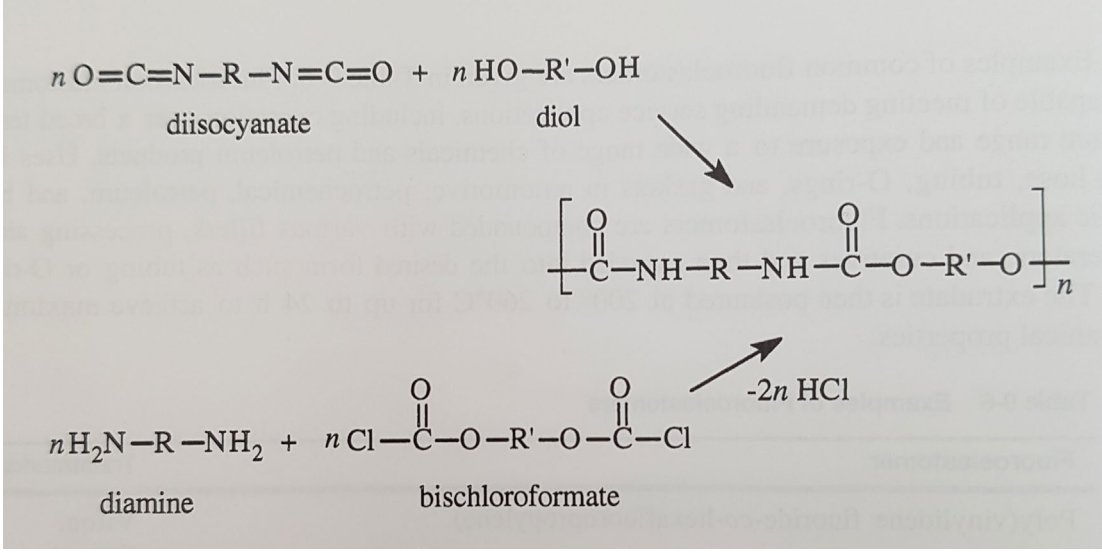

FIGURE 1. Routes to the synthesis of polyurethanes (Fried, 2003, 374)

As shown, the step growth polymerisation of diisocyanate with a diol occurs without liberation of low molecular weight by-product, unlike the bischloroformate reaction. The high reactivity of the isocyanate group enables polyurethanes to be processed by reaction injection molding. If either tri-isocyanates or compounds with multiple hydroxyl groups, or both of them are used for the process, is resulting polymer branched or bridged. (Seppälä, 1999,125)

Linear thermoplastic polyurethane is manufactured by diol reaction with diisocyanate. The melting point for resulting polymer is 175 - 183 °C. Thermoplastic polyurethane is used mainly for fibres having similar properties with polyamides.

3 SURFACE TENSION

Surface tension is one of the most important properties of liquids and solids. At the interface between a liquid and a gas, or between two immiscible liquids, forces develop in the liquid surface. These forces cause the surface behave as if it was a skin or a membrane. Although such skin is not actually present, this concept allows to explain several commonly observed phenomena. (Munson, 2010, 24)

This phenomenon is widely acknowledged in technology and in nature like droplets on metal surface or a leaf, capillary effect and water striders moving on a pond as in picture 1. This phenomenon is widely exploited in nature by plants and insects. They have inspired mankind to examine and utilize surface tension in modern technology.

PICTURE 1. Water strider (Sciphile.org)

The most ancient and well-known innovations utilising surface tension and especially decreasing surface tension is soap. There is recorded evidence that soaps were used for cleaning as far as 2800 BC in ancient Babylon. Most likely there has been traditional knowledge much longer but first written evidence dates back to 2200 BC. Still in the middle age, soaps were only used by upper class as production process was laborious and cost for soap was high. As chemical

industry evolved, ingredients for making soap were easier to manufacture. After this soap was no longer a luxury product.

3.1 Liquid and surface interaction

Liquid is a condensed phase which allows molecules to interact more than in gaseous phase. At the surface of a liquid molecules miss half of their interactions with homogenous molecules, which leads to unusual energetic state on molecule. As shown in figure 2 molecules at bulk interact to all directions with similar molecules.

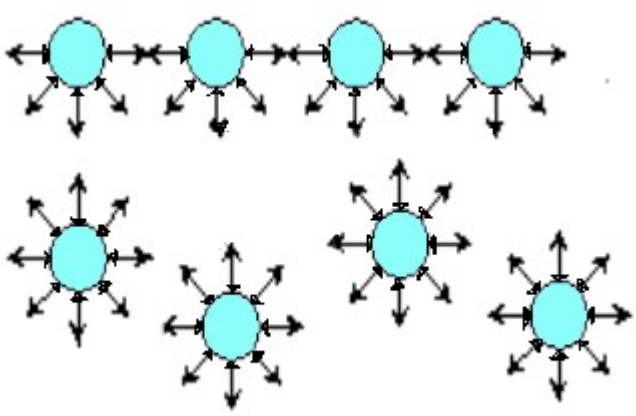

FIGURE 2. Intermolecular forces

However, the molecules in the liquid-vapor and liquid-solid interphase have different attraction and repulsion forces from bulk material and molecules from the other material. This causes energy equilibrium at the interphase which is seen as surface tension or surface energy for solids. It has been demonstrated that rough estimation of surface tension of liquids γ can be calculated with the formula 1.

$$\gamma \cong \frac{3N}{2^{10}} \frac{I}{d_m^2} \quad (1)$$

In this formula there are 3 different constants for liquid. N is the number of neighbour molecules, I is the ionization potential of the molecule and d_m is diameter of the molecule. As it is seen in formula 1, the surface tension for variety of liquids depends only on the potential of the ionization and diameter of the molecules. (Bormashenko, 2013, 5)

3.1.1 Wetting models

Wetting is an ability of a liquid to keep contact with solid surface on varying intermolecular forces when liquid is brought to contact with solid. The constitutional idea about wetting of solid was first expressed by Thomas Young in 1805. On his article, “An Essay on the cohesion of liquids”, he examined the correlation between contact angle and surface tension on ideal surface. When a droplet sits on a plain surface, three interfaces are linked in equilibrium contact angle of the liquid: solid-liquid (SL), liquid-vapor (LV) and solid-vapor (SV). as shown in figure 3.

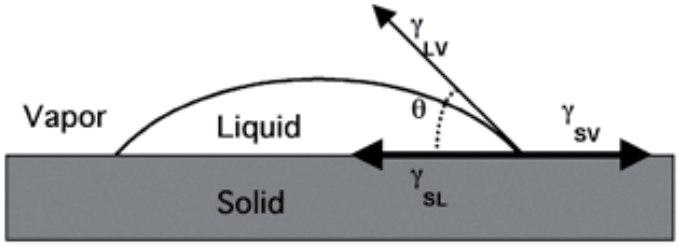

FIGURE 3. Liquid droplet on solid surface (Niemelä-Anttonen, 2015, 9)

These interfacial tensions can be described in Young’s equation (2)

$$\gamma_{SL} + \gamma_{LV} \cos\theta = \gamma_{SV}, \quad (2)$$

where γ_{SL} is the solid-liquid interfacial energy, γ_{LV} is the experimentally determined surface energy (surface tension) of liquid, θ is the contact angle and γ_{SV} is the surface energy of the solid. (Bormashenko, 2013, 13)

However, surfaces are rarely ideal as Young´s equation assumes. There is always either chemical heterogeneity or surface roughness present. Thus, Young’s equation was first modified by Wenzel in 1936 when he studied effects

of surface roughness on contact angle. In his studies Wenzel introduced roughness factor r, to describe the influence of roughness to θ on equation 3.

$$\cos\theta_W = r \cdot \cos\theta_Y \quad (3)$$

where θ_W is Wenzel contact angle on rough surface, r is roughness factor and θ_Y is ideal Young contact angle.

Later Cassie and Baxter modified Wenzel's equation by assuming there are two different areas beneath liquid droplet on rough surface. Their study result was Cassie-Baxter equation 4.

$$\cos\theta_{CB} = f_1 \cdot \cos\theta_Y - f_2 \quad (4)$$

where f_1 is surface area in contact with liquid and $f_2$is area in contact with air trapped beneath the droplet. The main differences of idea behind these three theories can be seen in figure 4. (Spori, 2008, 5411)

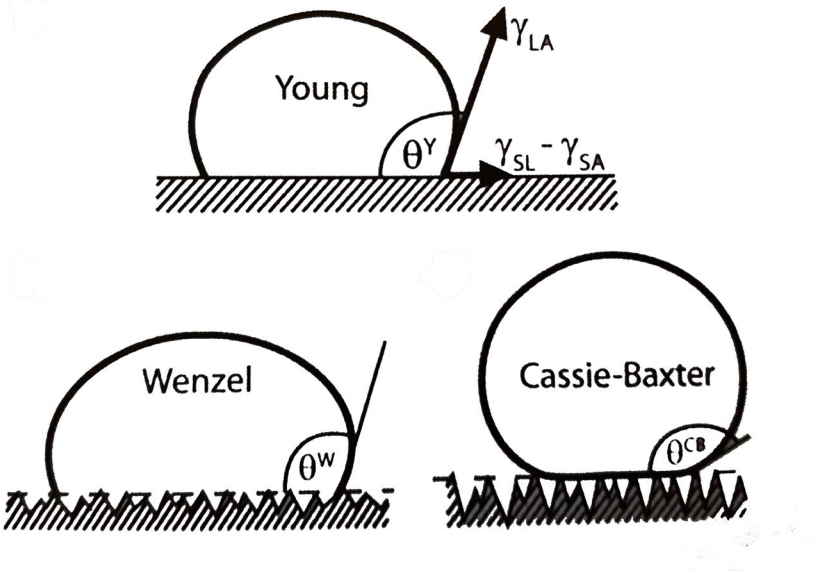

FIGURE 4. Wetting theories (Spori, 2008, 5411)

Wetting of the surface can be divided in three main categories as depicted in figure 5. The most common is partial wetting where water forms a cap on a surface. The easily measurable remark of cap is contact angle θ between the three phases of solid, liquid and gas. When 0° < θ < 90° for water, surface is called hydrophilic as in figure 5A. Another common scenario is depicted in figure

5B, where water spreads on the surface so evenly that no contact angle can be measured, i.e. complete wetting occurs. The third and most interesting scenario is complete dewetting 5C, phenomenon which is better known as superhydrophobicity. The surface is called superhydrophobic when CA θ > 150°. Superhydrophobicity will de discussed later in chapter 3.4. (Bormashenko, 2013, 13)

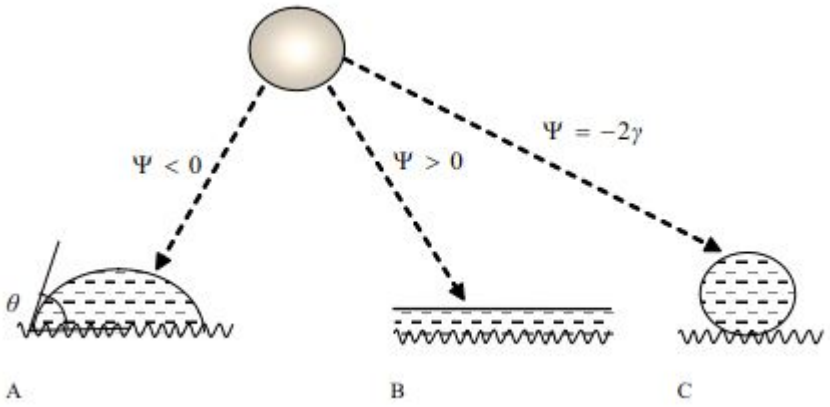

FIGURE 5. Wetting scenarios (Bormashenko, 2013, 13)

3.2 Contact angle

There are multiple different measurement methods developed for measuring contact angles. One simple method is optical goniometer where a droplet is placed on a sample surface. After illumination of droplet, the contact angle is examined with telescope or a camera. Nowadays telescope is connected to camera which gives more exact data than human eye ever could plausibly do. The principle of goniometric measurement is shown in figure 6 where a droplet is illuminated, and a camera is placed opposite to illumination source which takes picture from the droplet.

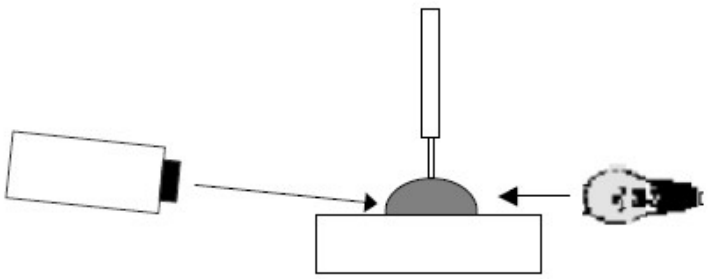

FIGURE 6. Principle of goniometer measurement (Krüss)

As goniometric measurement uses only small amount of liquid and most often small samples, there is a big possibility to impurities and human caused errors. Classically, when a droplet is almost flat, as on a hydrophilic surface, finding tangent line for measurement becomes challenging. Due the easy setup, goniometric measurement is well usable, unless extremely high accuracy is required. With modern cameras and computer software accuracy has increased considerably but there are still problems interpreting 2-dimensional results from 3-dimensional situation. (Yuan, 2013, 33)

3.2.1 Tilting plane method

In this method, a water droplet is slowly placed on a plane by a needle in order to avoid dynamic effects. The plane is then slowly tilted either manually or automatically and contact angles on the both sides of the droplet are measured. The sliding angle is the angle where droplet begins to move on the plane and there are three angles to be noticed: the advancing angle θ_A and receding angle θ_R, as illustrated in figure 7 and inclination of the plane.

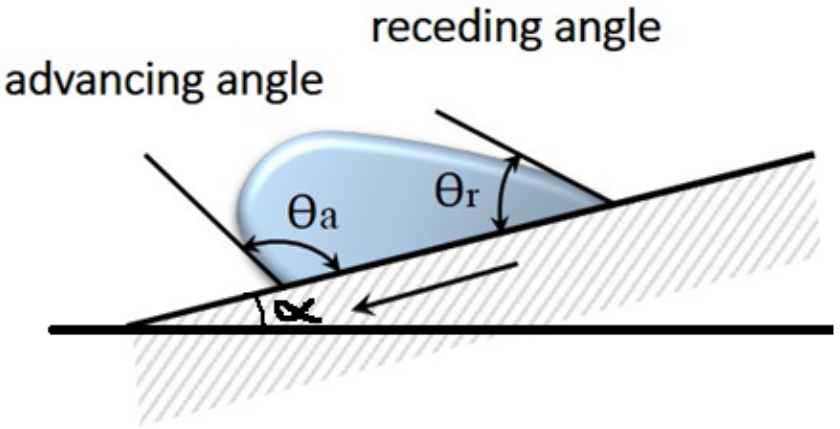

FIGURE 7. Contact angles on tilting plane (Weistron)

As shown in figure 7, three angles are present when measurement is performed by tilting plane method. First one is the angle of the surface with respect to horizon which is marked as α. On the droplet there are two different contact angles. The first one is on the side where droplet is about to move. This angle is so called

advancing angle θ_A. On the other side of the droplet is wider angle called as receding angle θ_R.

These three angles are expressed to have connection with each other by equation 5.

$$\sin \alpha = \gamma_l \frac{kR}{mg} (\cos \theta_R - \cos \theta_A), \quad (5)$$

where *k* and *R,* are constants depending on the drop, γ_l is the surface tension of the drop, *m* is the mass and *g* is gravitational constant. Another phenomenon called hysteresis is equivalent to the difference of advancing and receding contact angles. The tilting plane method gives good results if experiments are done with extreme care, but it is prone to human error in observation. (Bormashenko, 2015, 73)

3.2.2 Dynamic contact angle by sessile drop method

In order to examine more wettability related properties from the sample surface, the goniometric measurement can be considered as insufficient. Dynamic contact angle is a method where the size the contact angle of liquid is varied by increasing or decreasing sessile the liquid volume. While the droplet volume is changing, the advancing contact angle is measured while the volume is increasing, and correspondingly the receding contact angle is measured when the droplet is decreasing. The difference of these contact angles is called contact angle hysteresis.

There have been many studies on contact angle hysteresis phenomena and it has been confirmed that hysteresis is always present. Major causes for contact angle hysteresis include roughness and chemical heterogeneity of the surface but there are also other reasons mentioned in literature. In general, the problem of contact angle hysteresis is not completely solved. (Gindl, 2000, 280)

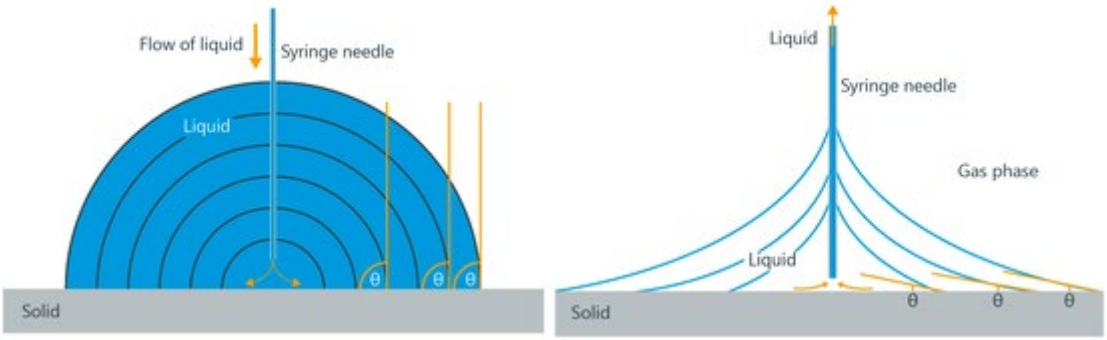

FIGURE 8. Illustration of hysteresis on sessile drop method (Krüss)

In figure 8 is illustrated the two measurement phases of dynamic contact angle. In first phase liquid droplet is brought onto surface. Syringe needle is positioned inside the droplet to keep flow of liquid as constant as possible. As liquid is brought into droplet it enlarges and contact angle θ between liquid and solid can be measured. On the second phase liquid is sucked from droplet causing change in droplet shape. This change in contact angle θ can be measured. Contact angle hysteresis can be easily calculated as difference between these two contact angles. If the hysteresis is small, the surface is flat smooth and homogenous. For larges hysteresis it can be expected to have roughness and heterogeneity in the solid surface.

3.3 Theoretical background of surface free energy

On solid particles, there is a series of cohesive forces between molecules. Inside the solid material a molecule attracts other molecules surrounding it and thus, it is affected by similar counterforces from other molecules. Due to this, resultant cohesive force inside the particle is non-existent. On the surface molecules are not surrounded by identical molecules and this causes a phenomenon called surface free energy (SFE). This phenomenon is close resemblance to surface tension observed on liquid surface.

The common way of obtaining surface energy for a solid material is measurement of contact angles for pure liquids with known surface tension parameters. The surface free energy γ_S of solid is the change of total surface free energy G per surface area A at constant temperature T, pressure P and amount of substance n as in equation 6.

$$\gamma_S = \left(\frac{\delta G}{\delta A}\right)_{T,P,n} \quad (6)$$

This characteristic property of solid material influences all surface related processes such as adhesion, absorption and wetting. The surface free energy, γ_S, of solid can be determined by measurement of contact angles of different liquids placed on the surface. However, the calculation of SFE from water contact angles has produced theories and equations for different materials. These equations are presented in following chapters.

3.3.1 Zisman approach

Major historical step in contact angle research was made by Zisman in 1964. In his study, "Relation of the Equilibrium Contact Angle to Liquid and Solid Constitution", he measured contact angles for different liquids on many low-energy solids. In the Zisman method contact angles θ for different liquids are measured and plotted as cosine θ versus surface tensions of corresponding liquids γ_L. Results were expressed as equation 7.

$$\cos\theta = 1 - b(\gamma_L + \gamma_s) \quad (7)$$

In this equation b is the slope of plotted regression line and γ_S is the surface energy of solid. Example of plotted Zisman method measurement is in figure 9.

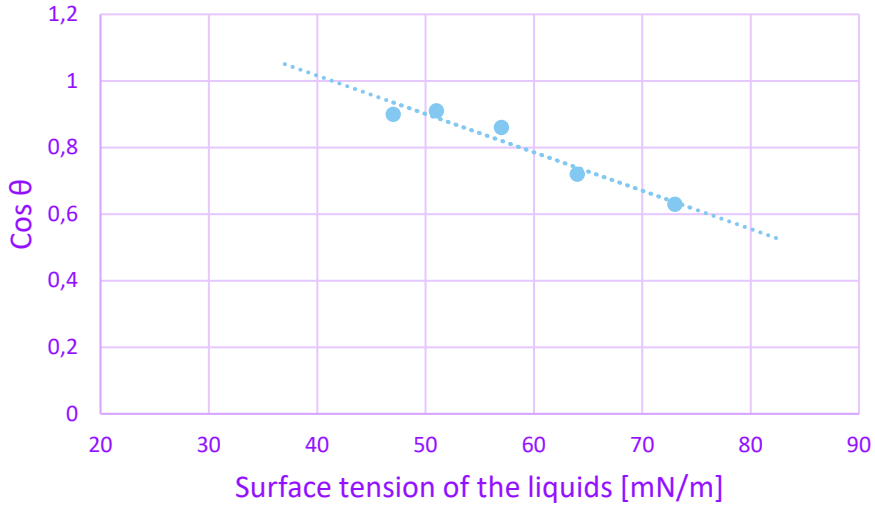

FIGURE 9. Zisman plot

During this work, he also brought the idea of critical surface energy γ_C where liquid fully wets the surface. If the measured values form a straight line in the plot, the full wettability is obtained by extrapolation to cos θ =1. At this point θ = 0 which obviously cannot be measured. (Gindl, 2001, 282)

After Zisman's pioneering work two major principles for measuring surface free energy evolved. Firstly, the equation of state approach which are identified as one liquid contact angle methods. Secondly SFE component approaches which are measured with two or more liquids.

3.3.2 Harmonic means equation (Wu's method)

In 1971, Wu proposed that intermolecular energy between two materials results from dispersion component and polar component of the energy. Due to the fact, that surface tension and surface free energy are proportional to intermolecular forces, it can be calculated as sum of components. SFE can be calculated as a summation of dispersion component γ_D and polar component γ_P. The energy between solid and liquid can be calculated as harmonic mean, as in equation 8.

$$\gamma_{SL} = \gamma_S + \gamma_L - \frac{4\gamma_S^d \gamma_L^d}{\gamma_S^d + \gamma_L^d} - \frac{4\gamma_S^p \gamma_L^p}{\gamma_S^p + \gamma_L^p} \quad (8)$$

In this equation γ_{SL} is the interfacial tension between solid and the liquid, γ_S is the surface energy of solid and γ_L is the surface tension of liquid. γ_S^d and γ_L^d are the dispersion components of SFE for solid and surface tension of liquid. γ_S^p and γ_L^p are the polar components of SFE and surface tension.

It was later found that surface energy values for polymers depend on the liquids used for contact angle measurements. For reliable results of SFE using harmonic mean equation, one is required to use pair of non-polar liquids. (Gindl, 2001, 282)

3.3.3 Equation of state approach (Neumann's equation)

Neumann's equation is based on equation of the state which assumes that work for adhesion in liquid-solid interface follows Berthelot's rule as in equation 9.

$$W_{SL} = \sqrt{\gamma_S \gamma_L} \tag{9}$$

In his studies Neumann derived Berthelot rule into equation of state for solid-liquid surface energy. This Neumann's equation 10 contains empirical constant β with value 0,000115 $(mN/m)^{-2}$

$$\gamma_{SL} = \gamma_S + \gamma_L - 2\sqrt{\gamma_S \gamma_L} \cdot e^{-\beta(\gamma_L - \gamma_S)^2} \tag{10}$$

When combining this theory with Young's equation there is a possibility to calculate SFE of solid by using only one liquid. This gives us the resulting Neumann's equation 11.

$$\cos\theta = -1 + 2\sqrt{\frac{\gamma_S}{\gamma_L}} \cdot e^{-\beta(\gamma_L - \gamma_S)^2} \tag{11}$$

Advantage of Neumann's equation is that only one liquid is needed for calculation of SFE but there is no possibility to evaluate dispersion or polar component of the energy. (Shimizu, 2000, 1832)

3.3.4 Owens-Wendt-Rabel and Kaelble method

In their studies Owens, Wendt, Rabel and Kaelble, later abbreviated as OWRK, expressed the idea that surface energy is the sum of different surface energy components, caused by intermolecular forces. Thus, the sum of surface free energy can be defined as in equation 12.

$$\gamma = \gamma_d + \gamma_H + \gamma_{di} + \cdots, \quad (12)$$

where γ_d is dispersion component, γ_H is hydrogen bonding component and $\gamma_{di}$is dipole-bonding component of energy. Most often this is reduced to equation 13

$$\gamma = \gamma_d + \gamma_N, \quad (13)$$

where γ_d is dispersion and γ_N is non-dispersion component of surface free energy. Resulting surface tension can be explained to be results of different molecular interactions such as polar interaction between dipoles like hydrogen bonding and dispersive interaction caused by charge fluctuation like van der Waals forces. It is necessary to use at least two different liquids for calculations: one polar and one non-polar liquid. From these measurements interfacial tension can be evaluated by geometric mean like in equation 14.

$$\gamma_{SL} = \gamma_s + \gamma_l - 2\left(\sqrt{\gamma_l^d \gamma_s^d} + \sqrt{\gamma_l^p \gamma_s^p}\right) \quad (14)$$

Combining this with Young´s equation gives us the OWRK equation 15.

$$\gamma_L(1 + \cos\theta) = 2\left(\sqrt{\gamma_l^d \gamma_s^d} + \sqrt{\gamma_l^p \gamma_s^p}\right), \quad (15)$$

where the values of γ_L, γ_l^d and γ_l^p can be easily measured or taken from literature. This method is universal for calculation SFE, but it is used especially for calculations on polymeric materials. (Haussler, 2016, 13)

3.3.5 Acid-base theory

Acid-base method is the most complex theory for evaluating SFE, but it also gives most information about details of surface free energy. In this theory SFE is seen as sum of dispersion component or van der Waals component γ_i^{LW} and polar component also known as Lewis acid-base component γ_i^{AB}. These acid-base components can be subdivided as in equation 16.

$$\gamma_i^{AB} = 2\sqrt{\gamma_i^+ \gamma_i^-}\,, \tag{16}$$

where γ_i^+ is electron acceptor parameter of acid-base and γ_i^- corresponding electron donor parameter of SFE components. When these are combined with Young's equation the acid-base theory can be obtained, as in equation 17.

$$\gamma_L(1+\cos\theta) = 2\left(\sqrt{\gamma_l^{LW}\gamma_S^{LW}} + \sqrt{\gamma_l^+\gamma_s^-} + \sqrt{\gamma_l^-\gamma_s^+}\right), \tag{17}$$

In order to determine SFE components γ_S^{LW} and parameters γ_s^+ and γ_s^- for the solid, the contact angle has to be determined at least with three liquids with known surface tension components. Also, two of these liquids should be bipolar. (Gindl, 2001, 282)

3.3.6 Comparison of the methods for SFE calculation

All the methods described earlier have their pros and cons for SFE calculations. Thus, all techniques have applications in research, depending on what kind of information is needed. Table 1 combines the information about the methods mentioned earlier. (Haussler, 2015, 11)

TABLE 1. Comparison of SFE calculation methods

Method	Minimum number of fluids	Advantages	Disadvantages	Applications
Zisman	2	Easy to implement	Obtained information is critical surface tension, not surface tension itself	Low surface energy
Neumann	1	Only one liquid required	Only surface tension obtained	Non-polar polymers
Wu (Harmonic mean)	2, at least one polar liquid	Different surface energy parameters obtained γ^p, γ^d		Low surface energy
OWRK	2, with one polar liquid	Different surface energy parameters obtained γ^p, γ^d		Polymers
Acid-Base theory	3, with 2 polar liquids	Most complete method obtaining surface energy parameters γ^+, γ^- and γ^{LW}	3 liquids with surface tension parameters required	polar and non-polar systems, biological systems

3.4 Superhydrophobicity

The phenomenon of superhydrophobicity was revealed in 1997 when W. Barthlott and C. Niehuis studied the wetting properties of number of plants and stated that the “interdependence between surface roughness, reduces particle adhesion and water repellence is the keystone in the self-cleaning mechanism of many biological surfaces”. Afterwards Barthlott studied a diversity of plants and

revealed a deep correlation between the surface roughness of plants, their surface composition and their wetting properties, varying from superhydrophobicity to superhydrophilicity. (Bormashenko, 2013, 116)

Superhydrophobic surfaces, which exhibit static contact angles with water larger than 150° and low CA hysteresis have attracted significant attention from both researchers and manufacturers. (Kulinich, 2011, 25) In nature there are various organisms that benefit from this phenomenon. For example, duck feathers repel water which enables the animal to fly after spending time in water. Reason for this ability is the microstructures in the feathers which makes the feathers to be superhydrophobic and thus prevents the water penetrate feathers as seen in figure 2.

PICTURE 2. Water droplets on duck feathers (Wikimedia)

The phenomenon of self-cleaning effect, which is also known as the lotus effect, is now one of the most studied phenomena in surface science. In picture 3, a lotus leaf possesses excellent water-repellent properties which allows them to clean themselves from dirt on surface. With this ability, the lotus leaf inhibits pathogens to reproduce on top of it, as the dirt is carried out with rolling water droplets. This also leads to self-cleaning ability of lotus leaf as rolling droplet gather all the dirt from the surface.

PICTURE 3. Lotus leaf (Max Pixel)

A visual example for hydrophobicity is illustrated in picture 4 where a droplet is resting on a polymeric coating, having water contact angle of 131°. If a surface has contact angle greater than 150 ° and hysteresis as low as 5° it allows droplet easily roll off the surface, thus being superhydrophobic.

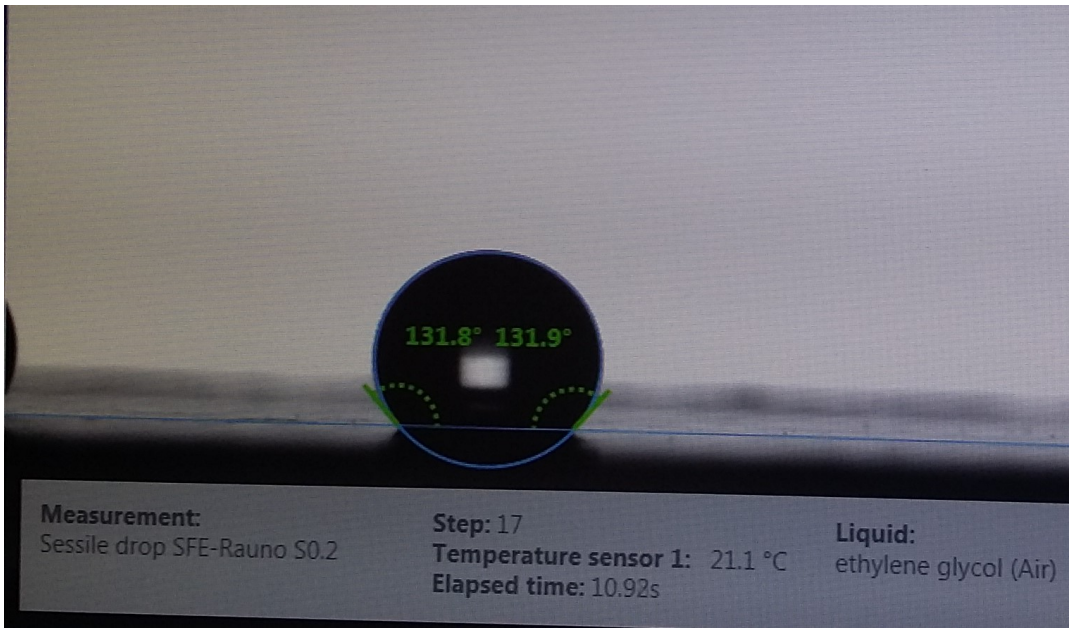

PICTURE 4. Contact angles on hydrophobic surface

Superhydrophobic surface exhibit extremely high water repellency, where water drops bead up on the surface, rolling with a slight applied force and bouncing if dropped on the surface from a height. It is now known that the degree to which solid repels a liquid depends upon two factors: surface morphology and surface energy. When surface energy is lowered, hydrophobicity is enhanced. Chemical

compositions determine the surface free energy and thus have a great influence on wettability. However, some limitations are encountered and superhydrophobic surfaces cannot be obtained only by lowering the surface energy. (Mohamed, 2014, 2)

In addition to high contact angles, superhydrophobic surfaces exhibit very low contact angle hysteresis, < 10°. Contact angle hysteresis is the difference between advancing and receding contact angle. This leads to rolling and bouncing of the water droplets, which will abolish particle contaminants from the surface leading self-cleaning property of superhydrophobic surface.

3.4.1 Nature inspired surface engineering

Examination of superhydrophobic phenomena has produced numerous of innovations during 18th and 19th centuries. The most known hydrophobic application was originally discovered by accident when scientists at DuPont were attempting to make new refrigerant. As tetrafluoroethylene was pressurized into a tank, it had polymerised causing nothing to come out. When tank was opened they found out that bottle was coated with extremely slippery polymeric material. This fluorinated material, later patented as Teflon™, has since then gathered wide use all over world in kitchenware as almost nothing sticks to it. This is caused by superhydrophobic nature of polytetrafluoroethylene.

Another phenomenon with close connection with surface tension of water is icing and preferably anti-icing. In the arctic regions, aviation, maritime logistics and powerlines icing causes major economical and energy losses as in picture 5.

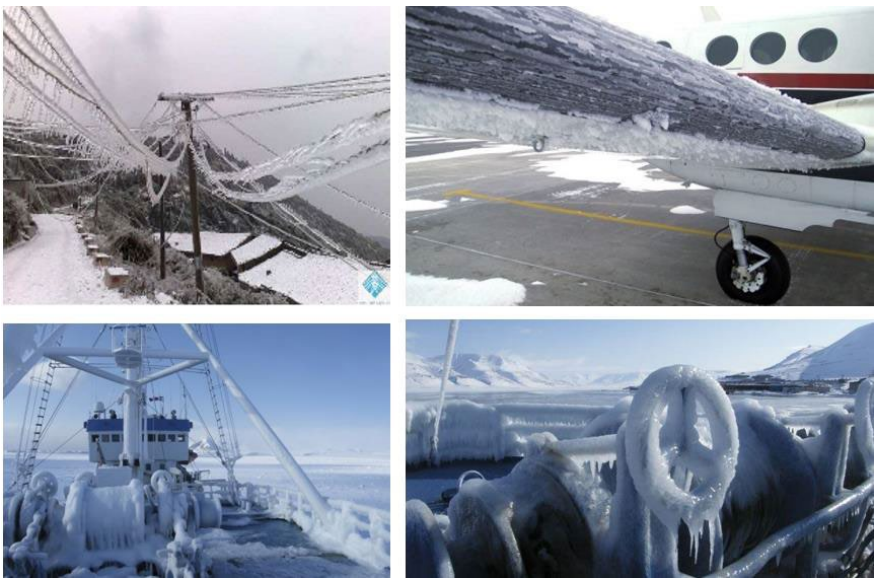

PICTURE 5. Problems caused by ice and frost

These challenges have inspired to investigate superhydrophobic and slippery innovations that are demonstrated to be less prone to icing than metallic materials. For example, in Tampere University of Technology icing research is carried out with icing wind tunnel and centrifugal ice adhesion test. The aim of the research is to find technological solutions that possess low ice adhesion strength in cold and wet conditions. One possibility to tackle icing might be so called SLIPS, slippery liquid-infused porous surfaces, which have exceptional liquid- and ice-repellence. The approach in SLIPS is inspired by the Lotus effect, but concept is different. Instead of air, the micro-structured substrates lock in place the infused lubricant fluid. They have shown to be hydrophobic as seen in pictuure 6 and they also have lower ice adhesion than normally used coatings. (Wong, 2011,443)

While the research of SLIPS has emerged during the last few years, the continuous fabrication of SLIPS over large areas in a cost-effective manner has not yet been demonstrated. This may be attributed to the difficulties in manufacturing large area substrates that have porous surfaces and affinity to preserve the fluorinated lubricant. These criteria limit the choice of substrates to intrinsically porous materials with low surface energy, e.g. porous Teflon nanofibrous mats or prepatterned films that have been surface modified with low surface energy chemicals. However, these requirements involve multiple tedious steps, including patterning, surface chemical treatment and lubricant coating. All

these restrictions have impeded the wider use of superhydrophobic surfaces and SLIPS. (Li, 2015, 23439)

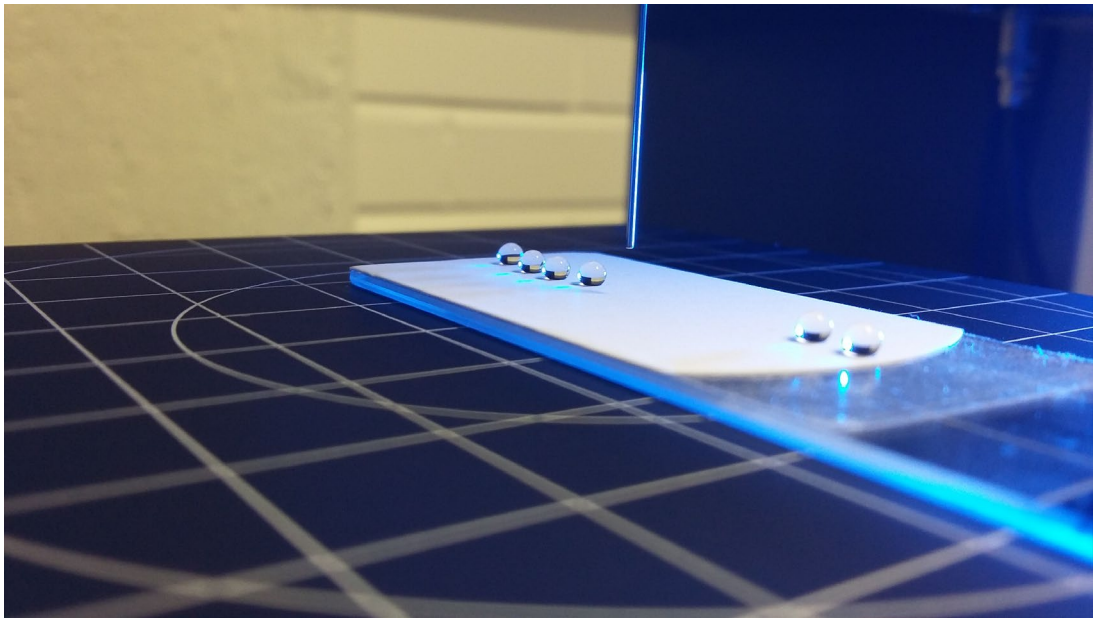

PICTURE 6. Water droplets on hydrophobic surface

3.4.2 Superhydrophobic polymer surfaces

Superhydrophobicity has drawn a great deal of attention from both fundamental and practical applications point of view. Although superhydrophobicity has been studied since the 1930s, interest in this phenomenon has grown this decade due to recognition of its potential applications in various areas. If superhydrophobic properties are impaired to fabric, one can make weather resistant fabrics and garments. (Kim, 2009, 235)

Due to their low surface energy, fluorinated polymers intrinsically exhibit strong hydrophobicity. For example, the water contact angle on a flat polytetrafluoroethylene surface is typically 115-120°. Roughening these surfaces leads to superhydrophobicity. One of the most widely used methods for fluorinated polymers is plasma etching. The high-energy oxygen species generated by plasma can etch polymer materials and create surface roughness needed to increase water contact angle up to 170°. The PTFE surface can also be roughened by simply stretching. The surface of PTFE films stretched more than 100 % of its original length consists of fibrous crystals with a large fraction of void space in the surface.

Another way is to use micro-phase separation of fluorinated block copolymers. The microphase separation of block copolymers can create a variety of nanoscale features needed for generation of superhydrophobicity. For example, a copolymer having equal amounts of methyl methacrylate monomers and fluorinated acrylate develops nanoscale pores at cast film surface during drying. By controlling film deposition parameters, the pore size much smaller than light wavelength can be produced, which makes the cast film optically transparent. (Kim, 2009, 244)

Polydimethylsiloxane (PDMS) is a hydrophobic polymer that can easily be processed to make rough surface textures. A high-power laser abrasion process has been used to make micro- and nano-scale structures. Laser abrasion processed PDMS surfaces have shown water contact angles higher than 160° and water sliding angle lower than 5°. Since PDMS can be processed as oligomeric liquid form and then cured into elastic solid by UV radiation, it is widely used to replicate surface textures of a mold. This process has been utilised to replicate the surface structure of lotus leaves and produce super hydrophobic PDMS surfaces. (Kim, 2009, 246)

4 EXPERIMENTAL PROCEDURES

4.1 Methods and materials

All the measurements for this thesis were performed between July and October 2017 with Krüss DSA 100S Drop Shape Analysis System located at Environmental Chamber Laboratory of Material science in Tampere University of Technology. The basic analysis system for most of measurements is seen in figure X below. The DSA 100 was equipped with tilting cradle unit which allows measurements of sliding angle and its hysteresis on inclined plane. All calculations for contact angles and surface energies were made by Krüss Advance 1.6.2.0 software which is partly seen in picture 7.

All measurements were performed with four equivalent samples of five different bulk polymer samples. Polymers used for measurements were polyethylene, ultrahigh molecular weight polyethylene (PE), polypropylene (PP), polytetrafluoroethylene (PTFE) and polyurethane (PU). The chosen polymers are common bulk polymers, which were used earlier in the laboratory for other studies and possess different surface energy and technical properties. Combining commercial accessibility and other well-known physical properties of hydrophobic polyolefins makes these materials attract great interest for research purposes. (Baba, 2015, 115)

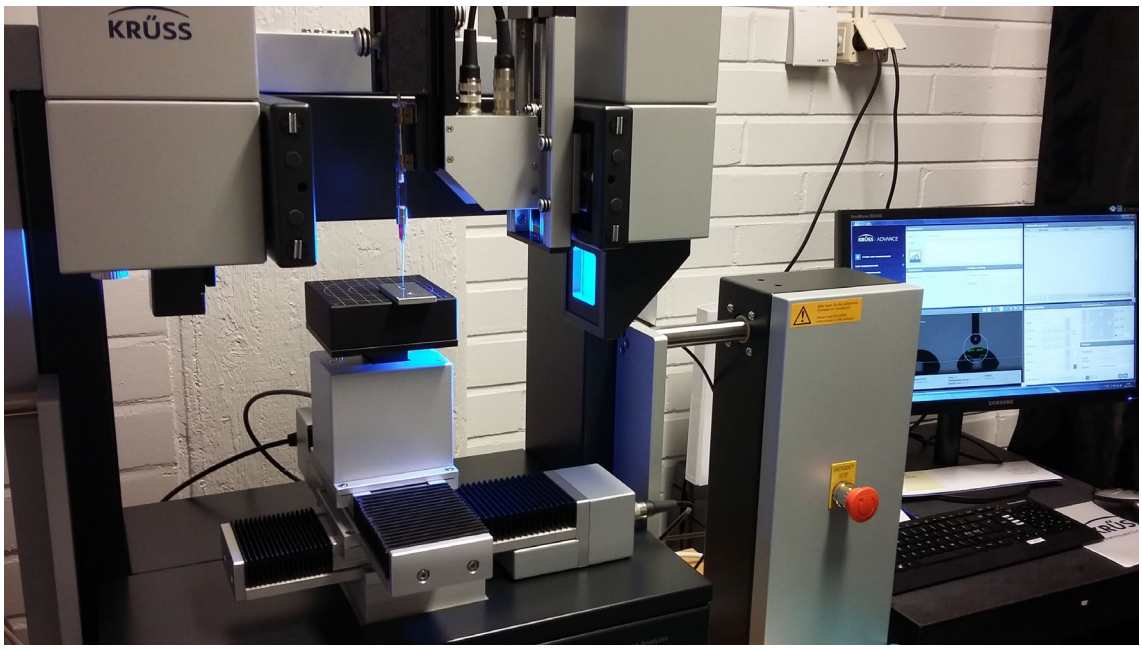

PICTURE 7. Krüss DSA 100S Drop Shape Analysis System

4.2 Contact angle measurements

All the measurements were performed with programmed automation process for minimising variables, e.g., in time and sample movement. Process was carried out in 5 - 7 loops to gather more data from each sample. This means that from every sample, 5-7 droplets were measured for further analysis. Example of this measurement program is shown in picture 8.

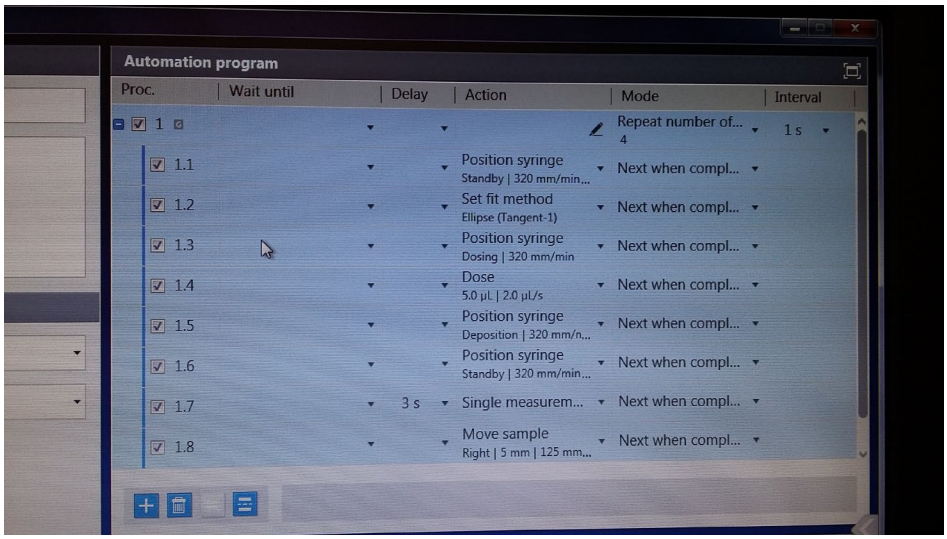

FIGURE 8. Measurement automation program

Three different liquids were used to yield data from samples, Milli-Q UHP water, ethylene glycol and diiodomethane, later abbreviated as DIM. DIM is poisonous

and sensitive to light so extra caution was needed for handling, storage and waste removal. Between measurements each sample was cleaned by wiping with absolute Ethanol AA.

4.2.1 Static contact angle for water

Before measurements 1000 µl glass syringe SY20 and steel needle were cleaned three times by spraying UHP water through them. Then the syringe was filled with water and attached to the syringe lifter unit. The polymer sample to be measured was placed on sample table below the needle.

Sample table was risen so that surface of sample was seen on camera screen in order to gain usable data from the samples. After this, the syringe lifter was lowered until the tip of the needle was seen on the camera. When the needle tip was seen, camera calibration was possible to perform. Width of steel needles, used for measurements, were exactly 0,50 mm. This calibration was necessary before each measurement, so Krüss Advance could scale data, obtained from each figure.

After the calibration, there were three needle positions to be set for the measurements. Standby position was the position where the needle was between all measurements, and dosing position was the height where droplet was formed. Deposition was the position where needle tip was in the proximity of sample and droplet was placed on the surface.

When needle positions were set and the calibration was done, sessile drop program was selected from template directory. After everything was set, Go-button was pressed in the bottom right corner to start automatic measurement. During measurement process Krüss DSA 100 produced six 5 µl water droplets and took four figures from each droplet with one second interval. Picture 9 is seen measurement process of contact angles for water on PU.

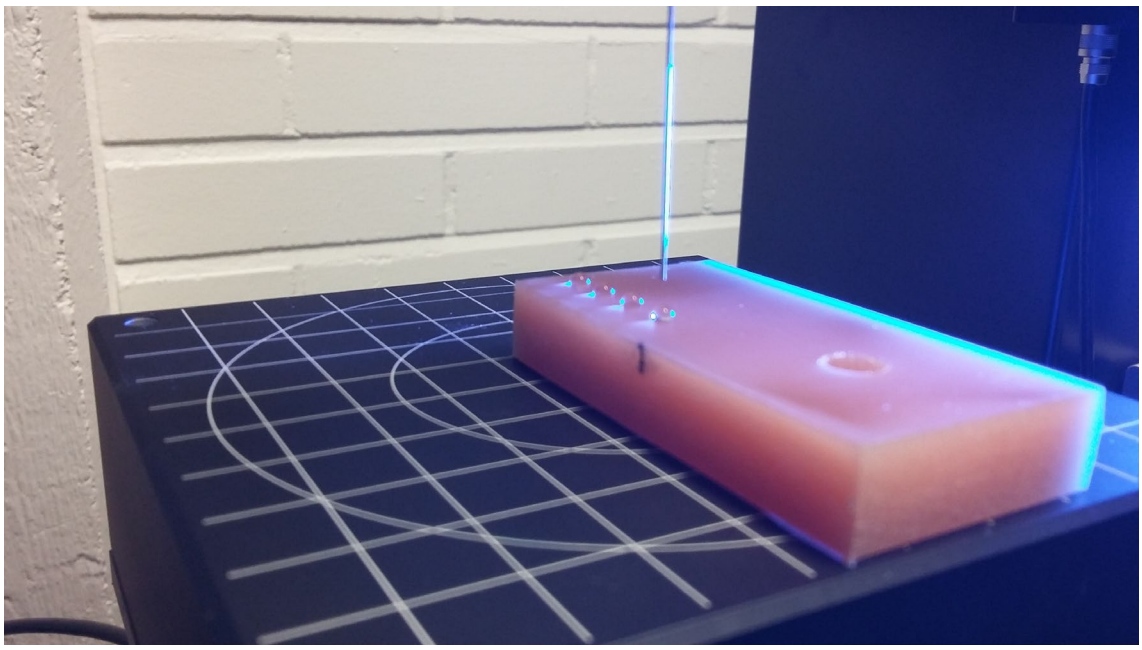

PICTURE 9. Contact angle measurement for polyurethane

When the automation process was done, all results and figures were examined for deviations and false data. If needed baseline correction for contact angle was done and deformed figures were removed from calculations. Calculated results for water contact angle (WCA) are expressed in table 12 at appendix 2.

If measurement was successful, new sample was set to sample table and measurement template was selected for new sample. After measuring all the samples, syringe lifter was lifted to safe height for handling, before detaching syringe safely. The syringe and the needle were rinsed with clean UHP water before they were set to drawer for further use. Quick manual for contact angle measurement is in appendix 1.

4.2.2 Static contact angle for ethylene glycol

For ethylene glycol measurements, abbreviated in tables as EtGl, measurement it was necessary to use disposable SY3601 1000µl syringes and PTFE needles, because viscosity of ethylene glycol makes it laborious to clean them. Before rinsing, it was necessary to measure width of needle for the calibration procedure, as the needle tip width varied between 0,57mm to 0,63 mm. After measurements,

the syringe and the needle were rinsed with ethylene glycol and filled with it. Due viscosity of ethylene glycol, air bubbles were easily formed into syringe, so this took always more than one attempt to fill properly. Syringe and needle were attached to syringe lifter. Polymer sample to be measured was placed on sample table below the needle. In the instrument configuration menu default settings were changed to SY3601 syringe and ethylene glycol as liquid for measurements.

Calibration process was performed as earlier mentioned for water measurement. After calibration was done, needle positions for automatic measurement process were set.

After everything was ready, measurement process and data analysis were performed as reported above in water droplet analysis.

4.2.3 Static contact angle for diiodomethane

For DIM measurement it was necessary to use disposable SY3601 1000µl syringes and PTFE needles. Before rinsing it was necessary to measure width of needle as it varied between 0,57mm to 0,63 mm. DIM is hazardous and sensitive to light so it was kept protected from light. Syringe and needle were rinsed with DIM and filled with it. Syringe and needle were attached to syringe lifter and polymer sample was placed on sample table below the needle. In the instrument configuration menu default settings were changed to SY3601 syringe and DIM as liquid for measurements.

Sample table was set as earlier for water and ethylene glycol measurements. When calibration was done needle positions for automatic measurement process were set.

After everything was set, the samples were measured, and the results were documented as described above in water droplet analysis.

When automatic measurement process was done, all results were examined. If needed corrections in baseline for contact angle was done and deformed figures were removed.

4.3 Surface free energy measurements

For the SFE calculations, contact angle measurements were performed with H_2O, ethylene glycol and diiodomethane. The usage of three liquids instead of two gave more for results as there were more variables. If there were deviation in SFE the reason for this is more easily found out with three different liquids.

All calculations of this study were made by OWRK sessile drop method as it was documented to be most suitable and most used for different polymer samples. As only the results obtained by same method are comparable, any notices with calculations using other methods were not taken. (Zenkiewicz, 2007,144) Results for SFE calculations are expressed in table 12 at appendix 2.

4.4 Sliding angle measurements

Sliding angle measurements were operated much like contact angle measurements with water but there was only one drop at the time on the sample. The polymer sample to be examined was fastened to sample table by two metallic clips to avoid sample slide out of sample table during measurement. This attachment is seen on picture 10 with running test on UHMW-PE.

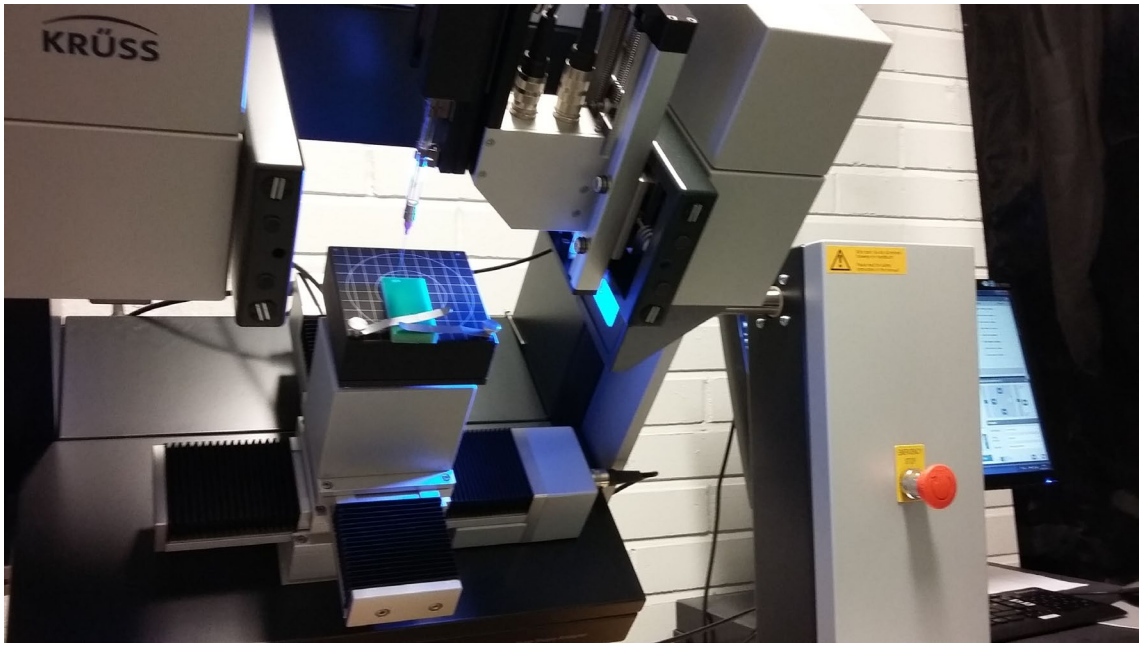

PICTURE 10. Sliding angle measurement

Automation process for sliding angle measurement was very straightforward. One 5 µl water droplet was produced onto the polymer sample. Tilting cradle was programmed to turn sample table 90° in 60 seconds. During this process, the camera took pictures every second and time when droplet began moving was recorded. Test was run twice for each sample. Results for sliding angle measurements are expressed in table 12 at appendix 2.

4.5 Experimental procedure for Peltier plate-measurements

Main emphasis of this work was to investigate possible correlation between temperature and SFE. For this work basic sample table was screwed off Krüss DS100 and replaced with TC40 Peltier plate-unit. Peltier plate unit has temperature element with a possibility to adjust temperature from -40 °C to 160 °C by external thermostat. The ambient atmosphere was replaced by N_2 as humidity in laboratory can influence the measurements. Thermostat liquid inlets and protective gas inlets explained in picture 11 below.

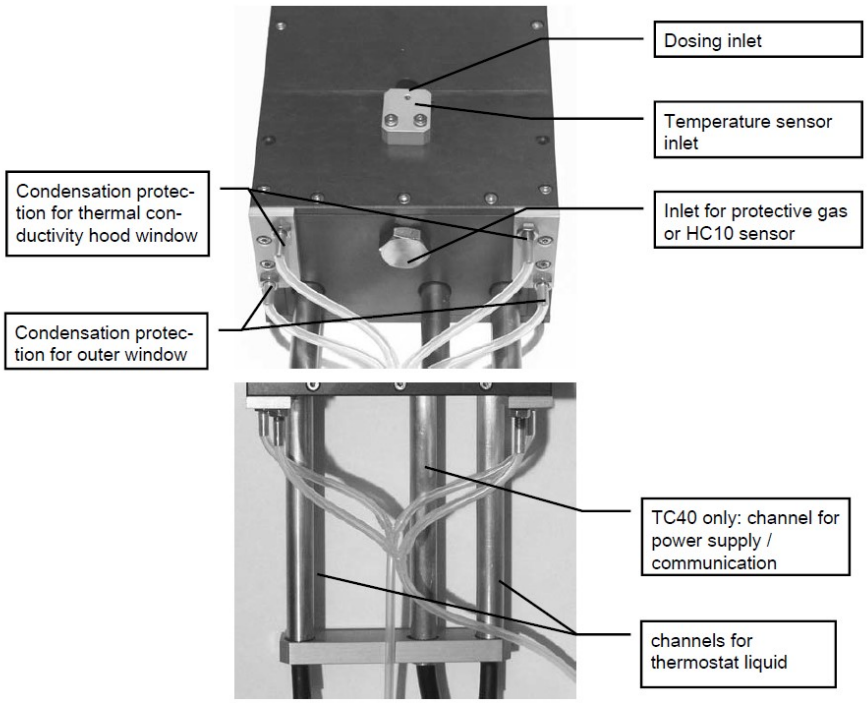

PICTURE 11. Inlets for Peltier plate-unit (Krüss)

As polymer samples were 6-8mm thick it was obvious that temperature of the peltier thermoelement is different than temperature at sample surface. For this reason, thermocouple attached to Fluke 51 II digital thermometer was mounted to measure sample temperature. Thermocouple was immobilized to structure by adhesive Bluetack® as in picture 12 before dosing inlet was sealed by laboratory film. The film was necessary to prevent excess humidity and heat transfer into and out from the measurement chamber.

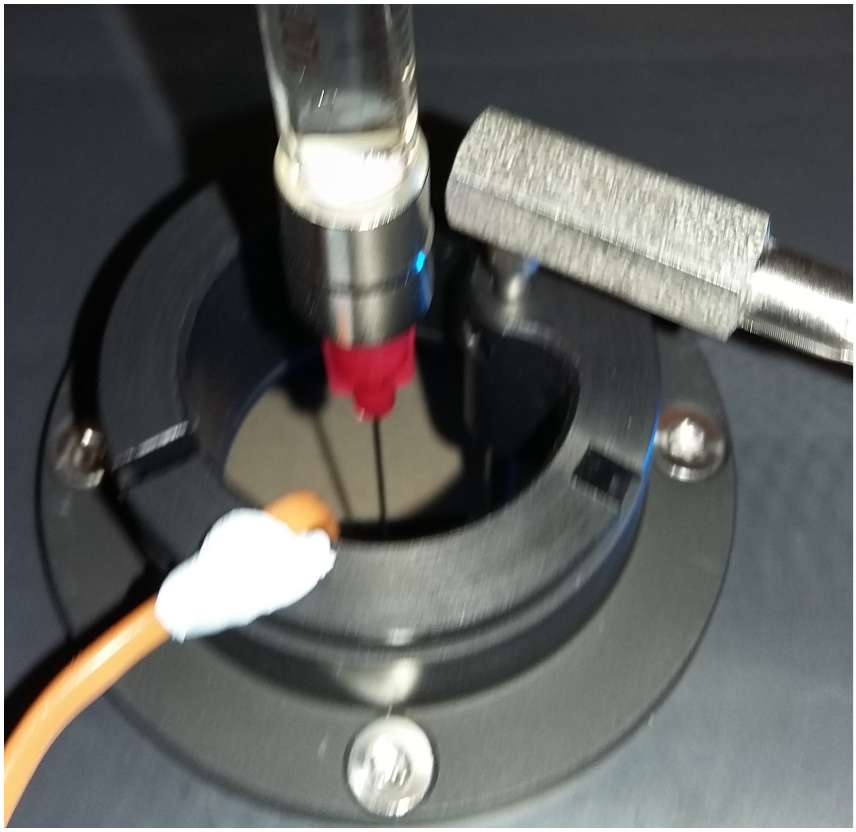

PICTURE 12. Bluetack®-immobilization of thermocouple

When the measurement chamber was sealed airproof and the camera calibrated as earlier described, the chamber was let to set until temperature was stable. Then automation process made a 5 µl droplet and after 60 second delay three figures were taken from the droplet. Sample was then moved with the screw on front of chamber to make another droplet to measure. This process was repeated once more to accomplish third droplet and total of 9 figures.

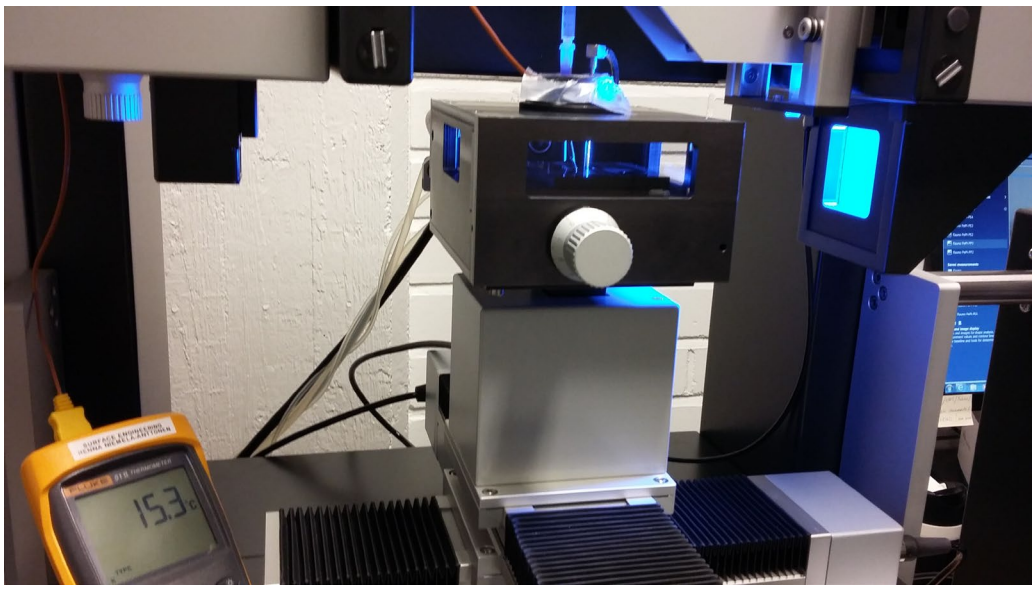

PICTURE 13. Setup for Peltier Plate measurements

After three measurements, the chamber temperature was decreased until the sample surface temperature was +15,0 ± 0,3 °C as seen in picture 13. While the environmental chamber and the sample were cooling, there was time to examine first measurements and make possible baseline corrections. After temperature had stabilized three droplets were made to be measured. Temperature was once again decreased to +10,0 ± 0,3 °C until it was stabilised, and third set of droplets were measured.

Once more chamber temperature was decreased and last measurements were made at +5,0 ± 0,3 °C. To speed up the later measurements for samples of same material, also temperature of cooling unit was recorded. Picture 14 shows the Krüss DSA100's own temperature sensor measuring temperature of the Peltier Plate and the Fluke thermocouple measuring the temperature of the sample surface.

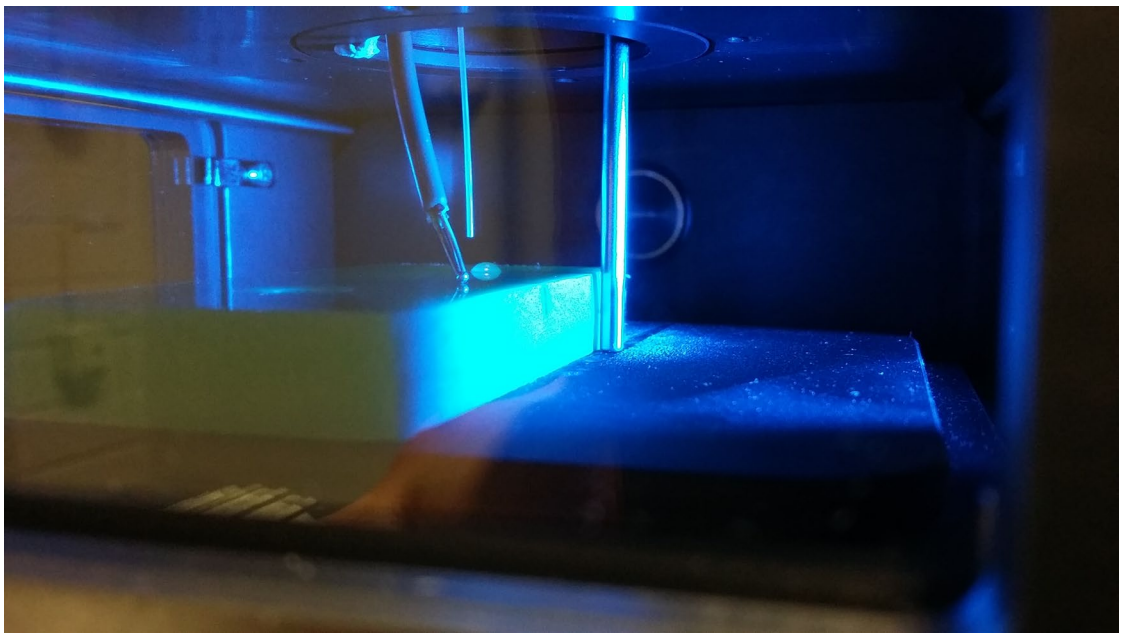

PICTURE 14. Thermocouple and temperature sensor inside environmental chamber

When measurements for all of the samples were done, the contact angles in each temperature were recorded. Also, the SFE at each temperature was also recorded for each sample. Average of CA and SFE for four parallel samples of each polymer were calculated. Measurement results in room temperature and +15 °C are expressed in table 13 at appendix 3. Measurement results in +10 °C and +5 °C are expressed in table 14 at appendix 4.

5 RESULTS

5.1 Static contact angle in room temperature

5.1.1 CA for water

Measurements for all samples were done with six 5µl H_2O-droplets and 4 pictures were taken from each droplet. Average result for each sample and average contact angles for each polymer type are listed in table 2. Distorted figures and figures with multiple droplets were discarded from calculations.

TABLE 2. Contact angles with UHP-H_2O

Polymer	sample 1	sample 2	sample 3	sample 4	average	std. deviation
PE	90	91	95	96	93	2,8
UHMW-PE	94	87	84	89	89	3,5
PP	96	97	99	97	98	1,3
PTFE	98	104	104	104	102	2,7
PU	109	100	95	97	100	5,2

Results for each polymer type were consistent as deviation of the results was only few percent. Only with PU1-sample deviation was 5 % of the average which is acceptable.
UHME-PE is slightly hydrophilic as CA is less than 90° and all other polymers are, more or less hydrophobic according these results.

5.1.2 CA for ethylene glycol

Measurements for all samples were done with six 5µl ethylene glycol and four pictures were taken from each droplet. Average result for each sample and average contact angles for each polymer types are listed in table 3. Distorted figures and figures with multiple droplets were discarded from calculations.

TABLE 3. Contact angles with ethylene glycol

Polymer	sample 1	sample 2	sample 3	sample 4	average	std. deviation
PE	65	66	68	70	67	1,6
UHMW-PE	70	64	62	62	64	3,2
PP	77	80	80	80	79	1,5
PTFE	87	82	88	76	83	4,6
PU	81	74	77	76	77	2,5

These results were also consistent as biggest deviation was 8 percent with PTFE4-sample. Contact angle for PU1 sample is once again higher than other polyurethane samples.

5.1.3 CA for diiodomethane

Measurements for all samples were done with six 5µl diiodomethane and four pictures were taken from each droplet. Average result for each sample and average contact angles for each polymer types are listed in table 4. Distorted figures and figures with multiple droplets were discarded from calculations.

TABLE 4. Contact angles with DIM

Polymer	sample 1	sample 2	sample 3	sample 4	average	std. deviation
PE	51	51	53	54	52	1,1
UHMW-PE	52	52	52	50	52	0,7
PP	56	59	60	62	59	1,9
PTFE	82	79	79	83	81	1,7
PU	55	50	51	44	50	3,9

Results for PE, UHMW-PE, PP and PTFE are excellent as deviations from average value is less than 3%. PU1 sample produces once again higher contact angle than other 3 PU samples. This time deviation was 10% from average. Due high CA of PU1 also the sample 4 differs highly from the average result.

5.2 Surface free energy

For surface free energy calculations, earlier reported contact angles were used for calculations. Average SFE for each polymer type was also calculated from separate sample SFE values. These results are shown in table 5.

TABLE 5. Surface free energies at room temperature $\left[\frac{\mathrm{mN}}{\mathrm{m}}\right]$

Polymer	sample 1	sample 2	sample 3	sample 4	average	std. deviation
PE	35	34,5	33	32,6	33,8	1,0
UHMW-PE	33,3	34,3	34,5	35,4	34,4	0,7
PP	27,2	29	27,3	27,4	27,7	0,7
PTFE	18,5	19,2	19,2	18	18,7	0,5
PU	31,2	34,5	33,7	33,6	33,3	1,2

Surface energies for all similar samples were close to each other, with the exception of PU1. As all contact angles measured for the sample were higher than average the resulting SFE for the sample in concern was lower than with other PU samples.

5.3 Sliding angle

For sliding angle measurements were run twice for each sample. Results are presented in table 6 below. If the droplet did not move before sample was tilted 90°, there is no remark in table 6. For UHMW3 result is from the only successful test, other numeric values are average of two tests results.

TABLE 6. Results for sliding angle measurements

	1	2	3	4
PE	-	-	-	-
UHMW-PE	-	69	76	71
PP	69	54	54	-
PTFE	-	-	-	-
PU	-	-	-	-

As it can be seen there were successful measurements only for UHMW-PE and PP. Even for those samples it results were not obtained for all parallel measurements. PTFE and PU did not give any results which was controversial to CA measurements. It was assumed for these samples to have smaller sliding angle than PP.

5.4 Peltier plate-measurements

Peltier plate tests were the slowest ones to perform and the biggest interest was also on the relationship between temperature with water contact angle and SFE. Because of that, the main emphasis of the results is on these tests. Peltier plate

tests were run on the calendar period of 7.7.-29.9.2017. For each result 3 water, ethylene glycol and DIM droplets were made, and 3 figures was taken out of each, resulting average of 9 individual results from which average was calculated.

5.4.1 Peltier plate measurements for PE

Test results of water contact angle (WCA) and SFE for polyethylene samples and the average result for polyethylene are listed below in table 7.

TABLE 7. Peltier plate results of polyethylene samples

	+21°C		+15°C		+10°C		+5°C	
	WCA	SFE	WCA	SFE	WCA	SFE	WCA	SFE
PE1	88	32,3	77	32,6	85	34,2	81	34,0
PE2	87	33,4	75	32,6	73	35,4	77	34,1
PE3	84	33,7	76	33,2	64	38,7	70	41,1
PE4	82	32,3	76	30,5	67	33,3	72	34,2
PE-average	85	32,9	76	32,2	72	35,4	75	35,9

The relationship of water contact angle and temperature is expressed in figure 10 below. As can be seen from the figure 10, there is slight trend of contact angle decreasing when temperature goes down.

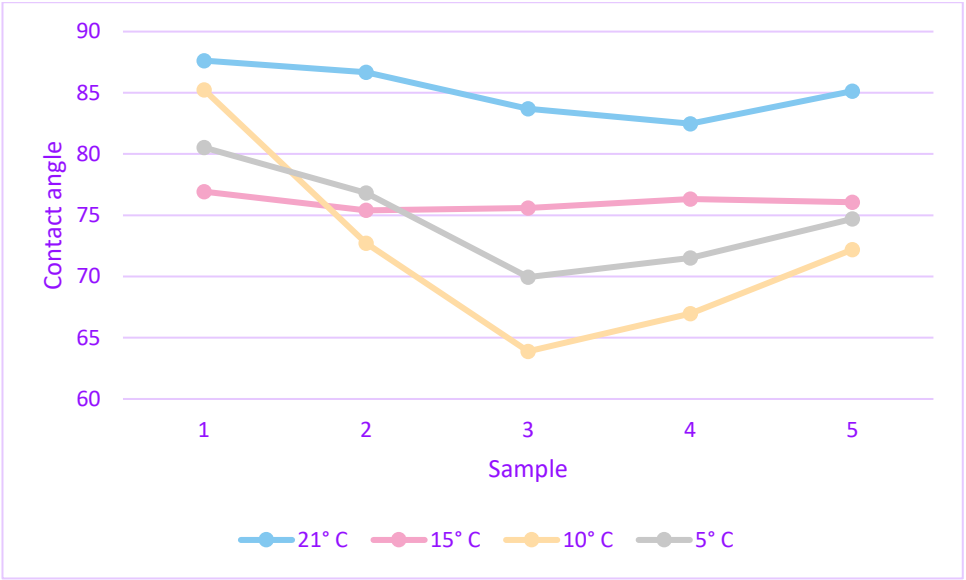

FIGURE 10. Water contact angle for polyethylene with Peltier plate

The relationship on SFE of polyethylene and temperature is expressed in figure 11. The trend of surface energy increasing with temperature decreasing is not completely clear.

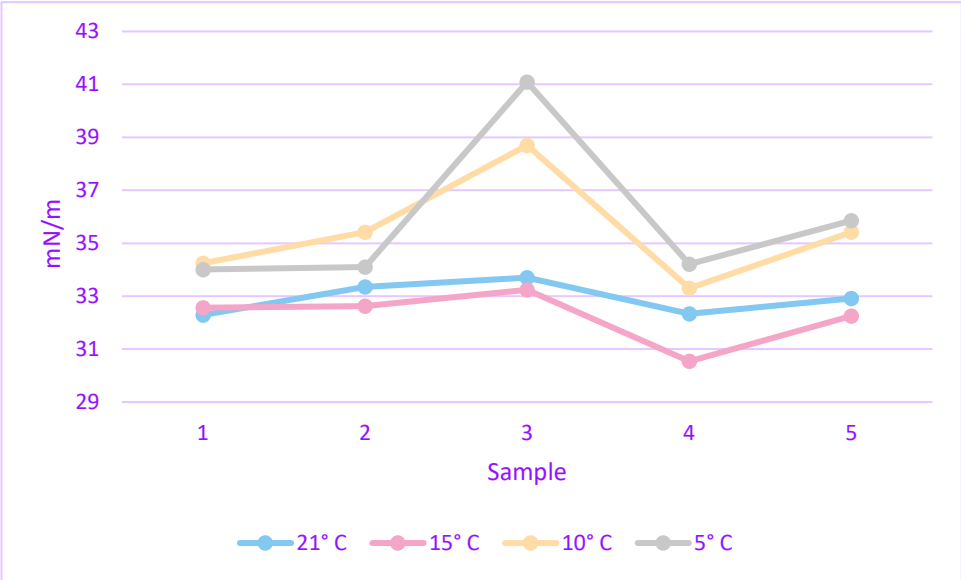

FIGURE 11. Surface Free Energies for polyethylene with Peltier plate

5.4.2 Peltier plate measurements for UHMW-PE

Test results of water contact angle and SFE for UHMW-PE samples and the average results for UHMW-PE are listed below in table 8.

TABLE 8. Peltier Plate test results for UHMW-PE

	+21°C		+15°C		+10°C		+5°C	
	WCA	SFE	WCA	SFE	WCA	SFE	WCA	SFE
UHMW-PE1	81	33,0	77	32,9	74	33,2	72	33,9
UHMW-PE2	85	32,6	78	33,7	76	34,0	75	33,1
UHMW-PE3	85	33,1	77	33,7	73	39,8	74	37,0
UHMW-PE4	83	34,0	78	35,0	71	33,3	73	39,7
UHMW-PE av.	83	33,2	77	33,8	73	35,1	73	35,9

Figure 12 shows a trend of water contact angle decreasing with temperature. Some zig-zagging to be noticed at lower temperatures.

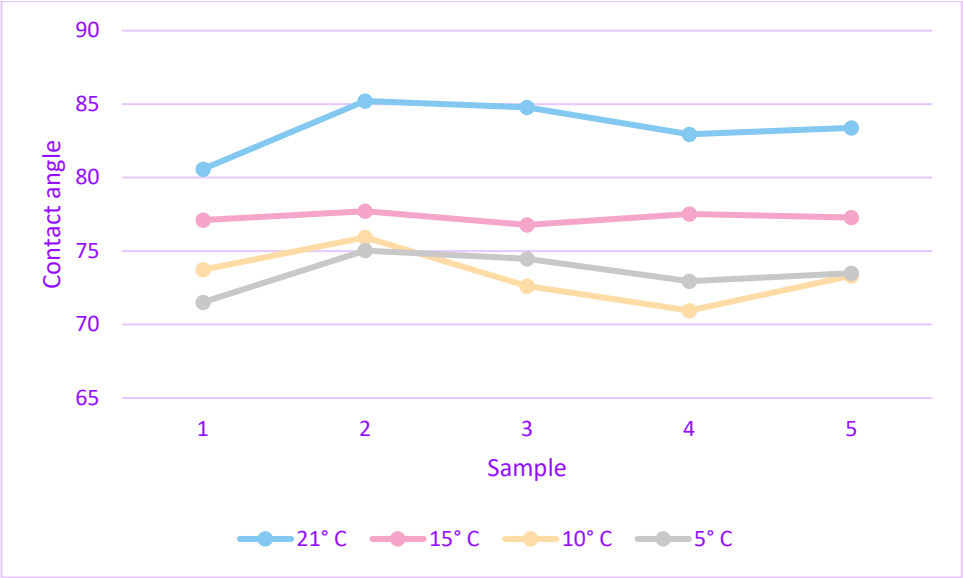

FIGURE 12. Water contact angle for UHMW-PE with Peltier plate

In Figure 13 is expressed the changes of SFE in correspondence to temperature. As one can see there is some inconsistency with the results at +10° C.

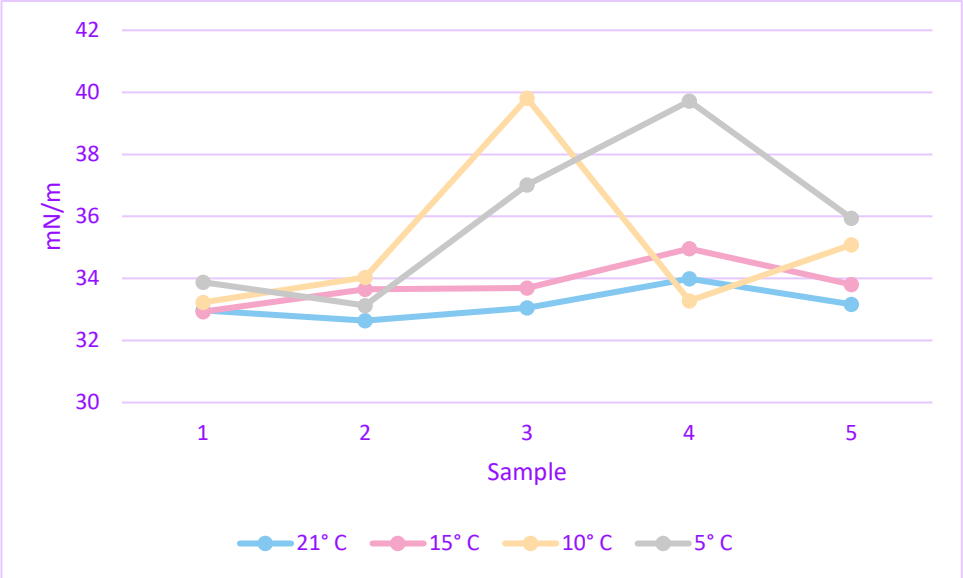

FIGURE 13. Surface Free Energies for UHMW-PE with Peltier plate

5.4.3 Peltier plate measurements for PP

Test results of water contact angle and SFE for polypropylene samples and the average result for PP are listed below in table 9. Results for sample 1 are lower than other results throughout measurement process.

TABLE 9. Peltier Plate test results for PP

	+21°C		+15°C		+10°C		+5°C	
	WCA	SFE	WCA	SFE	WCA	SFE	WCA	SFE
PP1	91	31,2	93	30,3	88	30,2	85	28,5
PP2	93	31,3	95	29,7	94	29,9	89	30,5
PP3	92	30,6	94	30,4	90	30,4	89	30,9
PP4	95	29,8	95	29,0	93	28,5	90	28,7
PP-average	93	30,7	94	29,9	91	29,8	88	29,6

There is obvious trend of water droplets spreading more on the PP surface when temperature decreases. Only inconsistency is that contact angles at ambient temperature were smaller than at +15° C. Relationship of temperature and WCE of PP is expressed in figure 14.

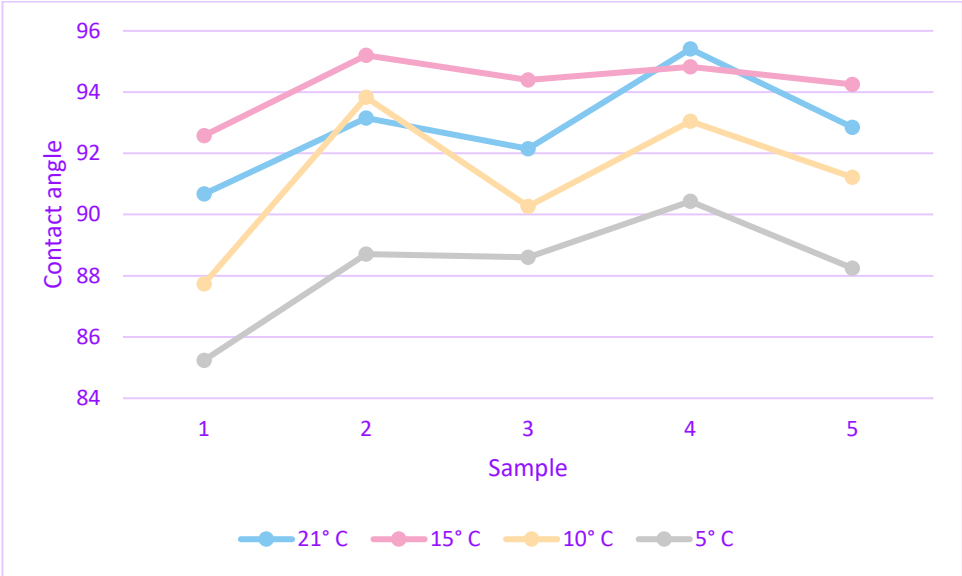

FIGURE 14. Water contact angle for PP with Peltier plate

The results for surface free energy of PP in relationship with temperature are not as clear as wished based on water contact angles. Especially +5 °C results were inconsistent when compared with higher temperatures. This trend curves are shown in figure 15 below.

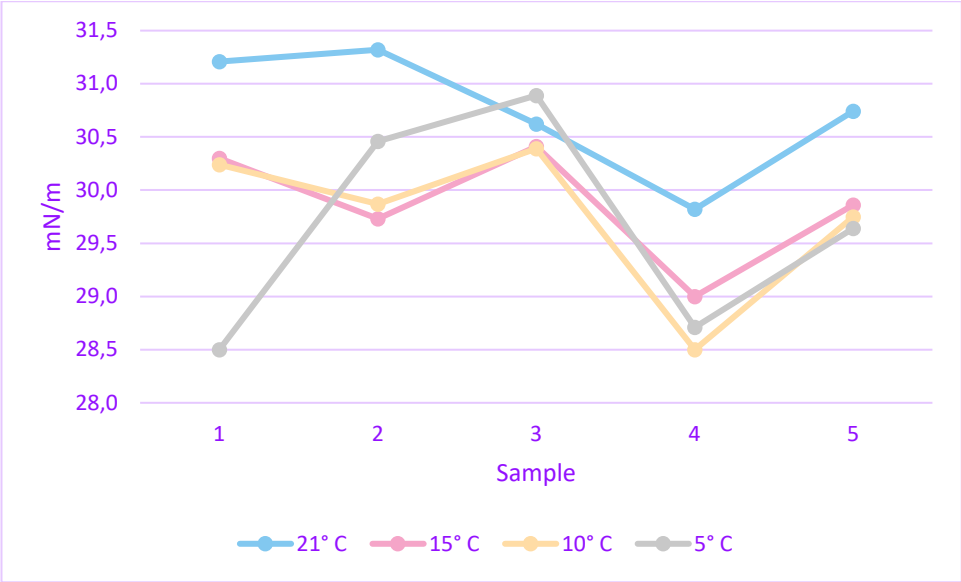

FIGURE 15. Surface Free Energies for PP with Peltier plate

5.4.4 Peltier plate measurements for PTFE

Test results of water contact angle and SFE for polytetrafluoroethylene samples and the average result for PTFE are listed below in table 10. Results for PTFE sample 1 and 3 are a bit inconsistent, especially the contact angles in ambient temperature were low.

TABLE 10. Peltier Plate test results for PTFE

	+21°C		+15°C		+10°C		+5°C	
	WCA	SFE	WCA	SFE	WCA	SFE	WCA	SFE
PTFE1	94	18,5	101	19,2	92	20,7	92	19,9
PTFE2	100	17,2	89	17,0	90	16,6	89	17,5
PTFE3	92	16,7	91	18,8	92	17,7	90	21,6
PTFE4	100	15,7	93	17,5	92	17,4	92	18,2
PTFE-av.	96	17,0	94	18,1	91	18,1	91	19,3

The zig-zag trend of water contact angles at room temperature can be clearly seen in figure 16. The highest measured contact angle at +15°C does not fit to the trend of decreasing contact angle with lowering temperature.

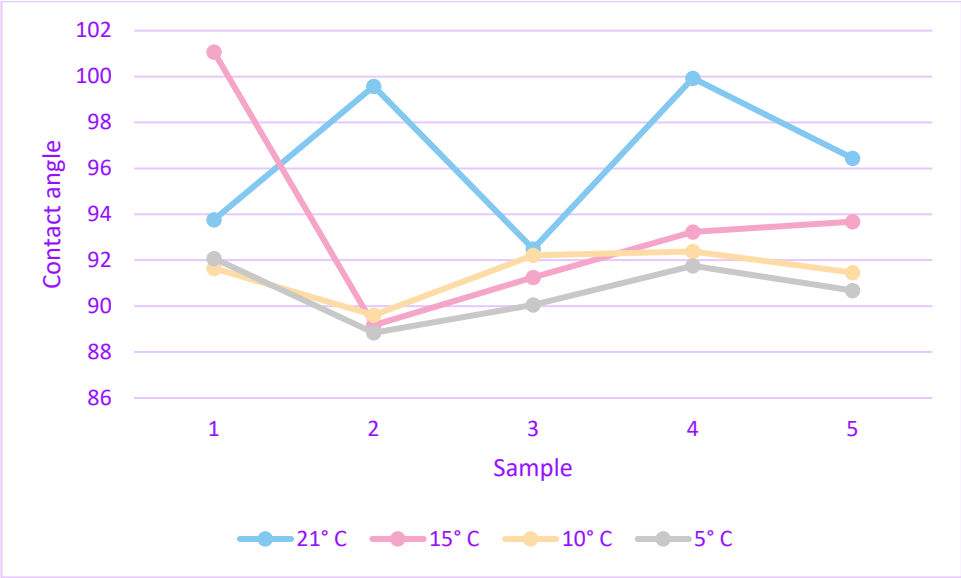

FIGURE 16. Water contact angle for PTFE with Peltier plate

The inconsistency of the results can also be seen with the results of surface free energy especially with sample 2 in figure 17. The SFE on PTFE sample 3 at +5°C in exceptionally high compared to others but the contact angles with ethylene glycol and DIM did not give clear explanation.

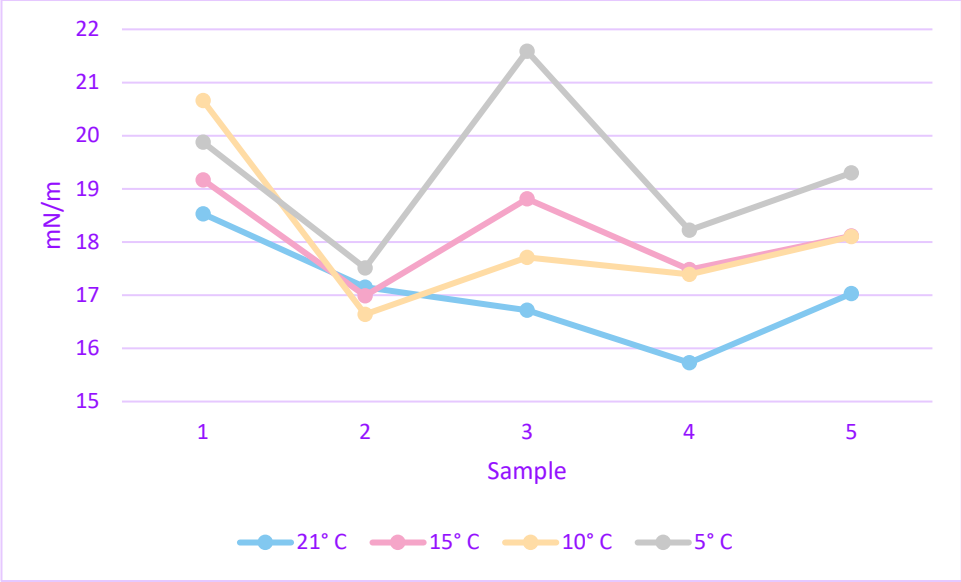

FIGURE 17. Surface Free Energies for PTFE with Peltier plate

5.4.5 Peltier plate measurements for PU

Test results of water contact angle and SFE for polyurethane samples and the average result for PU are listed below in table 11. It is noticed that contact angles are drastically decreasing when temperature is decreased.

TABLE 11. Peltier Plate test results for PU

	+21°C		+15°C		+10°C		+5°C	
	WCA	SFE	WCA	SFE	WCA	SFE	WCA	SFE
PU1	97	31,7	78	26,9	75	35,4	65	33,1
PU2	87	37,5	78	34,6	73	37,0	77	30,9
PU3	87	35,3	82	36,9	72	37,1	67	44,9
PU4	91	28,6	78	22,2	67	39,2	68	41,1
PU-average	90	33,2	79	30,2	72	37,2	69	37,5

The trend curves of polyurethane water contact angles are unambiguous. While temperature decreases, water droplet spreads more to the surface. as seen in figure 18.

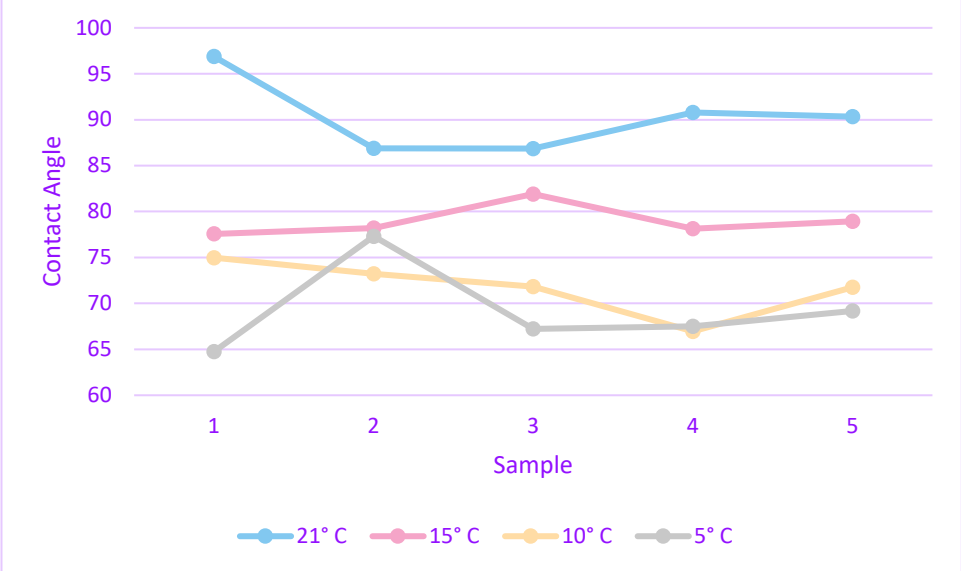

FIGURE 18. Water contact angle for PU with Peltier plate

The surface free energy measurements for polyurethane did not give as distinct results as results were with water. The most suspicious result is with sample 2 which is measured to have lowest SFE at +5°C which is opposite to the trend with other samples. These results are seen in figure 19 below.

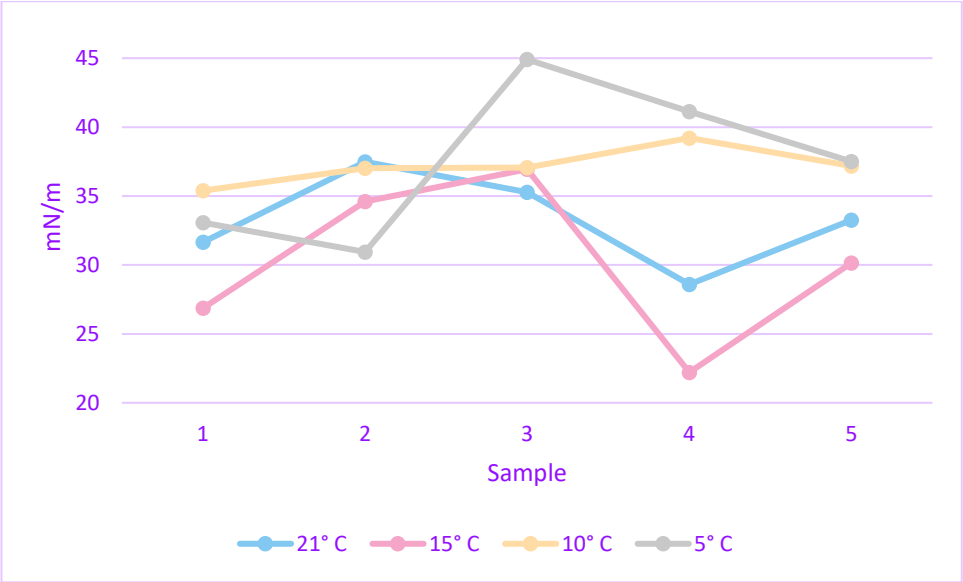

FIGURE 19. Surface Free Energies for PU with Peltier plate

6 DISCUSSIONS AND CONCLUSIONS

It can be seen from the results and figures that there is correspondence on the temperature and contact angles as well as temperature with surface free energy. This was noticed as contact angles for water, ethylene glycol and diiodomethane were systematically smaller when temperature was lowered from room temperature. When surface free energy was calculated from the observed contact angles, it was noticed to rise when temperature was lowered from room temperature.

There is still need for more research and development in experimental process to get more unambiguous results for scientific purposes. The materials for testing process were not ideal as the cooling process took most of the time on Peltier plate measurements. Impurities on samples caused background distortion as seen in picture 15. Distortion caused unbalanced and smaller contact angles compared to the angles measures on actual surface. Due this every single image had to be examined and corrected if needed. As this research was made with limited amount of samples, there is no enough statistical data to make mathematical formula of correlation between temperature and surface free energy of polymer samples.

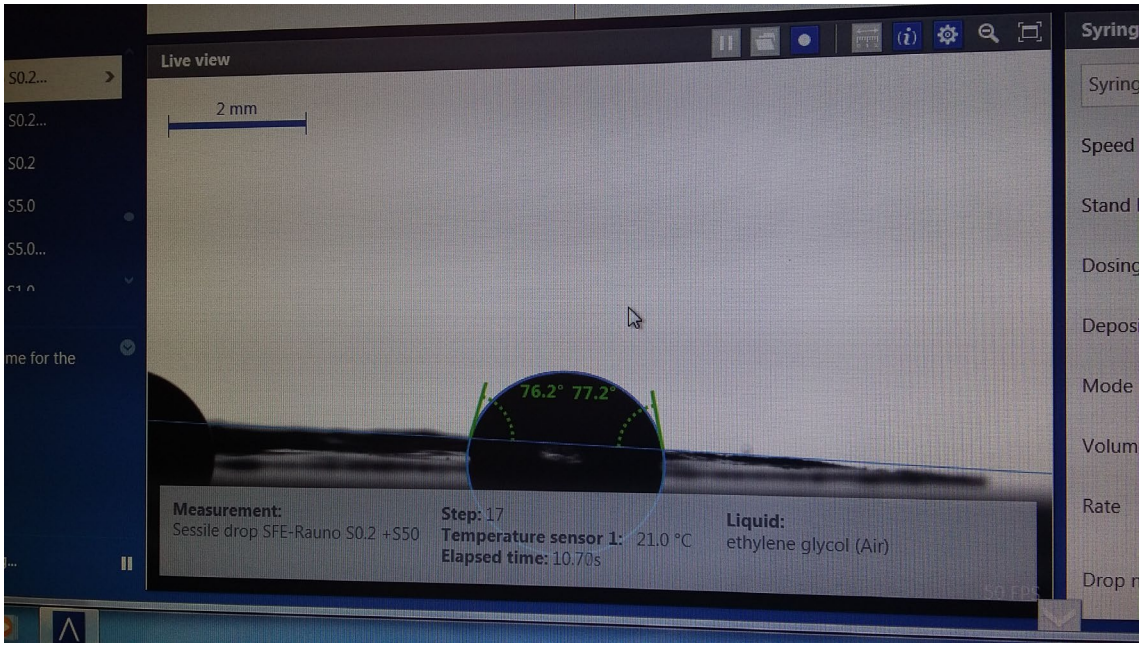

PICTURE 15. Background distortion

The environmental chamber used for Peltier plate measurements was problematic compared to normal sample table. Samples had to be moved manually inside the chamber in order not to break syringes. This manual transportation allowed only 2-3 droplets to be measured before chamber had to be opened. Due to this, humidity was transported to the chamber and long waiting periods were necessary for N_2-atmosphere to be present inside chamber. If this was not done properly moisture condensed on the samples as seen clearly in picture 16. Obviously results with condensed water as in picture 16 could not be used as small droplets caused incoherent background.

PICTURE 16. Condensed water

At lower temperatures moisture caused another visible problem if N_2-atmosphere was not present. The temperature of the cooling plate had to be lower than the desired measurement temperature for cooling to be efficient.

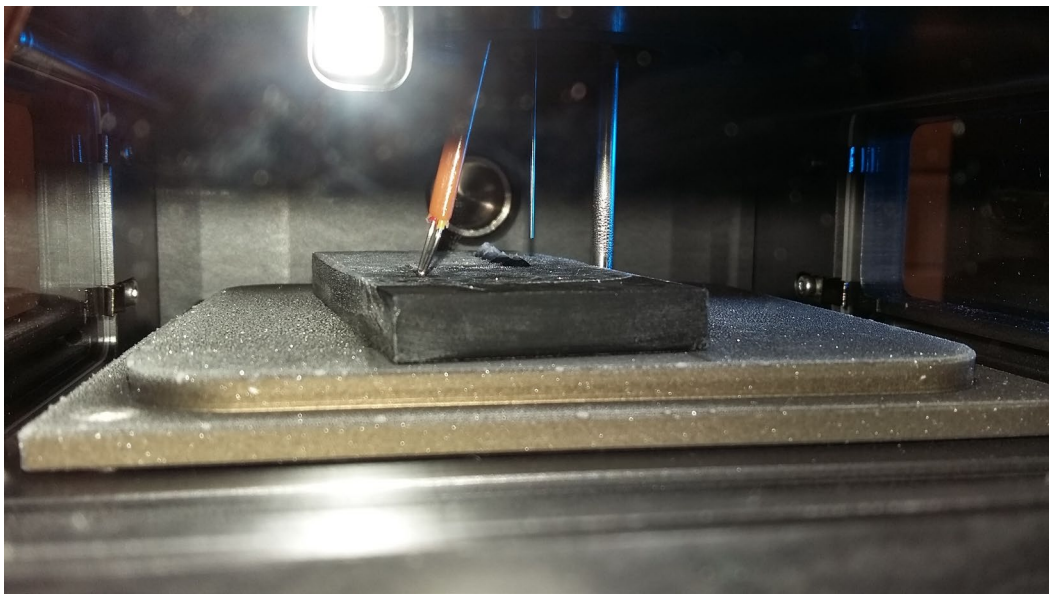

PICTURE 17. Frozen sample

As it can be seen in picture 17, the quick cooling process with moisture caused frost on the sample and droplets were changed into ice peaks during 60 second delay between droplet formation and measurement. Naturally these results were not used as droplets did not have the shape they normally would have.

The measurements with PU were the most problematic. There were at least three reasons to suspicious results. PU samples were about 2 mm thicker than the other polymer samples which caused it to take lot more time during cooling processes with Peltier plate unit. There were also visible changes in surface structure of the samples as some parts of surface were glossy and others were matt coloured. This could be the reason for problems seen in picture 18.

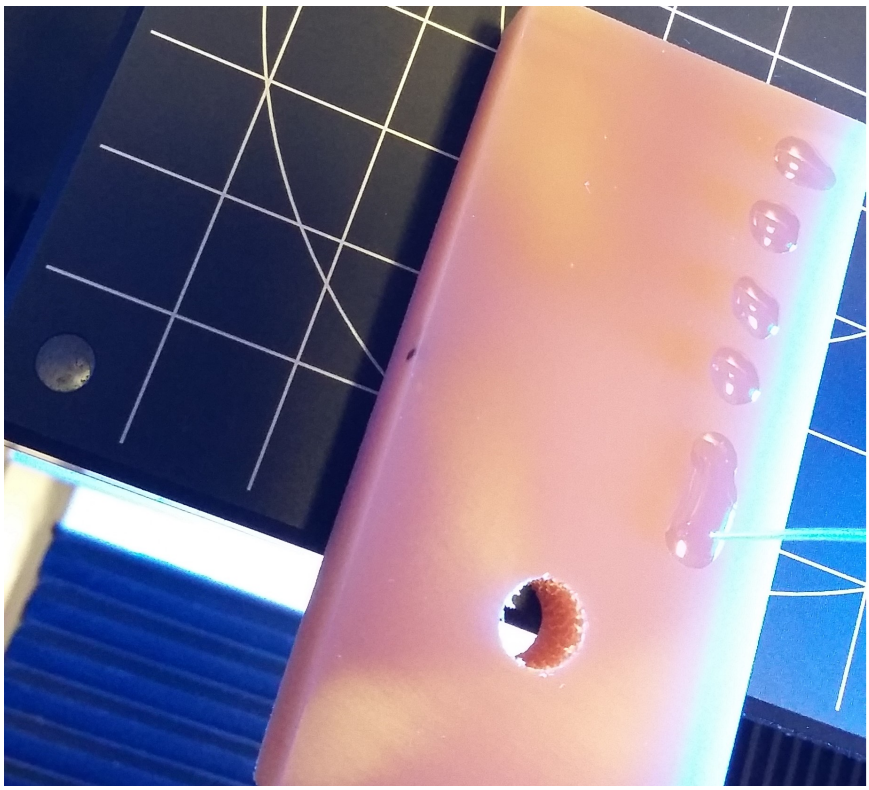

PICTURE 18 Distorted droplets on polyurethane

None of the 6 droplets in picture 18 is ideally round and two droplets have merged with each other. Due this the actual shape of droplet was not completely seen in camera causing Krüss Advance giving which are difficult to decode. This kind of problems could be avoided if DSA had camera unit taking pictures from above, and thus giving 3-dimensional picture from the droplet. When performing measurements with Peltier plate, even this would not solve the problem, as the droplets are in a small chamber with no line of sight from above.

For the future study, humidity in environmental chamber is most critical problem to be solved for Peltier plate measurements in low temperature. As the Peltier plate chamber needed to be opened during measurement procedure, which allowed moist air to replace N_2-atmosphere in the chamber. Other possible solution is to use only one droplet per temperature, and three measurement temperatures. This way opening of the chamber during measurements could be avoided. On the other hand, obscurity of the results would rise, as those would be only from one point of the sample.

Another major modification for the future, is in sample preparation. The ideal polymer samples to be examined are much thinner than the ones used in the

study. This would speed up the measurement process as the sample temperature would result from thermoelement instead of measurement atmosphere.

As a conclusion contact angle analysis is usable method of measuring surface free energy in low temperatures, as long as the samples are specifically prepared to be suitable for Peltier plate measurements and problems caused by humidity are solved. There is a noticeable trend for samples to have smaller contact angles and thus higher surface free energy when temperature is lowered.

REFERENCES

Baba, E. M., Cansoy, C. E. and Zayim. E. O. 2015. Optical and wettability properties of polymers with varying surface energies. Applied Surface Science 350 (2015) pp 115-120 http://dx.doi.org/10.1016/j.apsusc.2015.02.150

Bormashenko, E. Y. 2013. Wetting of Real Surfaces. Berlin: De Gruyter.

Bruice, P.Y. 2003. Organic Chemistry. 3rd ed. Upper Saddle River, NJ: Prentice Hall

Fried, J.R. 2003. Polymer Science and Technology. 2nd ed. Upper Saddle River, NJ: Prentice Hall

Geyer, R., Jambeck, J. R., and Law, K. L. 2017. Production, use, and fate of all plastics ever made. Science advances, *3*(7), e1700782. doi:10.1126/sciadv.1700782

Gindl, M., Sinn, G., Gindl, W., Reiterer, A. and Tschegg S. 2001. Colloids and Surfaces A: Physiochemical and Engineering Aspects 181, pp 279-287

Haussler, A. 2016. Wettability. MSC Thesis work. University of Limoges

Kim, S. H. 2008. Fabricating Superhydrophobic Surfaces. Journal of Adhesion Science and Technology, 22(3-4), pp 235-250, http://doi.org/10.1163/156856108X305156

Krüss DSA100 Drop Shape Analysis System: Installation and operation. 2010. Hamburg: Krüss GmbH

Kulinich, S.A., Farhadi, S., Nose, K. and Du, X.W. 2011. Superhydrophobic surfaces: Are They Really Ice-repellent?. Langmuir, 27, pp 25-29

Li, Y., John, J. Kolewe, K. W., Schiffman, J. D. and Carter, K. R. 2015. Scaling Up Nature: Large Area Flexible Biomimetic Surfaces. ACS Applied Materials and Interfaces. 7 (42), pp 23439-23444, https://pubs.acs.org/doi/abs/10.1021/acsami.5b04957

Mohamed, A. M. A., Abdullah, A. M. and Younan, N.A. 2015. Corrosion behaviour of superhydrophobic surfaces: A review. Arabian Journal of Chemistry. Vol 8(6), pp 749- 765. https://doi.org/10.1016/j.arabjc.2014.03.006

Munson, B.R. 2010. Fundamentals of Fluid Mechanics. 6th ed. Hoboken, NJ: John Wiley & Sons

Niemelä-Anttonen, H. 2015. Wettability and Anti-icing properties of slippery liquid infused porous surfaces. MSc Thesis work. Tampere University of Technology

Seppälä, J. 1999. Polymeeriteknologian perusteet. Helsinki: Otatieto Oy

Spori, D.M., Drobek, T., Zürcher, S., Ochsner, M., Sprecher, C., Mühlebach, A. and Spencer, N.D. 2008. Beyond the Lotus Effect: Roughness Influences on Wetting over a Wide Surface-Energy Range. Langmuir, 24, pp 5411-5417

Shimizu, R. N. and Demarquette, N., R. 2000. Evaluation of surface energy of solid polymers using different models. Journal of Applied Polymer Science Vol 76. pp 1831-1845

Weistron Instruments. 2014. http://www.weistron.com/products/contact-angle-meter

Wong, T-S., Kang, S. H., Tang, S. K. Y, Smythe, E. J, Hatton, B. D., Grintal, A. and Aizenberg, J. 2011. Bioinspired self-repairing slippery surfaces with pressure-stable omniphobicity. Nature, vol 27. pp 443-447

Yuan, Y. and Lee T. R. 2013. Surface Science Techniques. Berlin: Springer Berlin Heidelberg.

Zenkievicz, M. 2007. Methods for the calculation of free energy of solids. Journal of Achievements in Materials and Manufacturing Engineering Vol 24. Issue 1. pp 137-145

APPENDICES

Appendix 1. Quick manual for Krüss DSA 100

1. Turn on power from switch behind DSA
2. Start Krüss Advance on computer and choose appropriate measurement mode
3. Choose measurement template or start new measurement (bottom right corner)
4. Take applicable syringe and needle for your work. Glass syringe for water and, disposable plastic syringe for other liquids
5. Rinse syringe 3 times and needle twice with solvent
6. Fill the syringe and attach needle. Open clamping screw and lift dispenser with lower slider (Ctrl+Backspace) to desired height, where plunger fits the holder slots.
7. Seat the syringe and tighten clamping screw.
8. Place your sample on sample table
9. Lower the syringe with slider (Ctrl+Backspace) so that you see tip of needle in camera.
10. Click calibration. (figured as tape measure)
11. Move blue vertical bars to edges of needle and horizontal bar above tip of needle. Focus image to needle.
12. Type to Object size-box width of needle (0.5 mm for water). Click Calibrate.
13. Type your measurement program and/or draw sample map. (pictures 19 and 20)
14. Begin measurement (bottom right)
15. Scroll down monitor to check results. Click on deviant results and check/correct baseline (manual baseline- overwrite). Tick off marking on deformed figures.
16. Scroll down and move your results as excel/pdf to flash drive for further analysation
17. Lift the syringe to safe height, loosen the clamping screw detach syringe.
18. Rinse glass syringe and needle with water. Put back to drawer.
19. Clean up your mess!

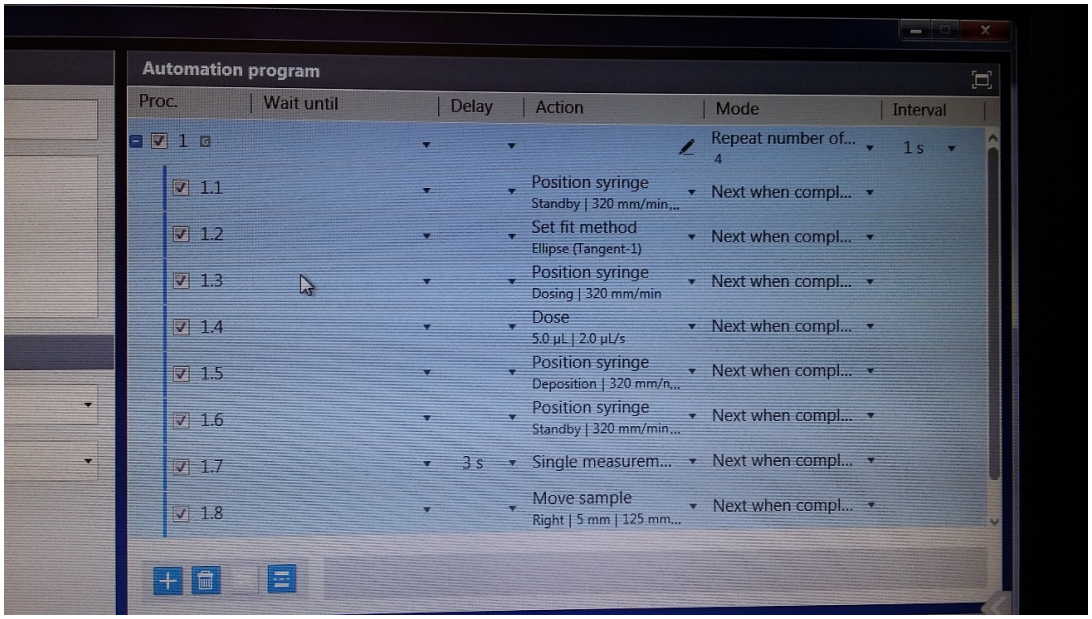

PICTURE 19. Example of measurement program

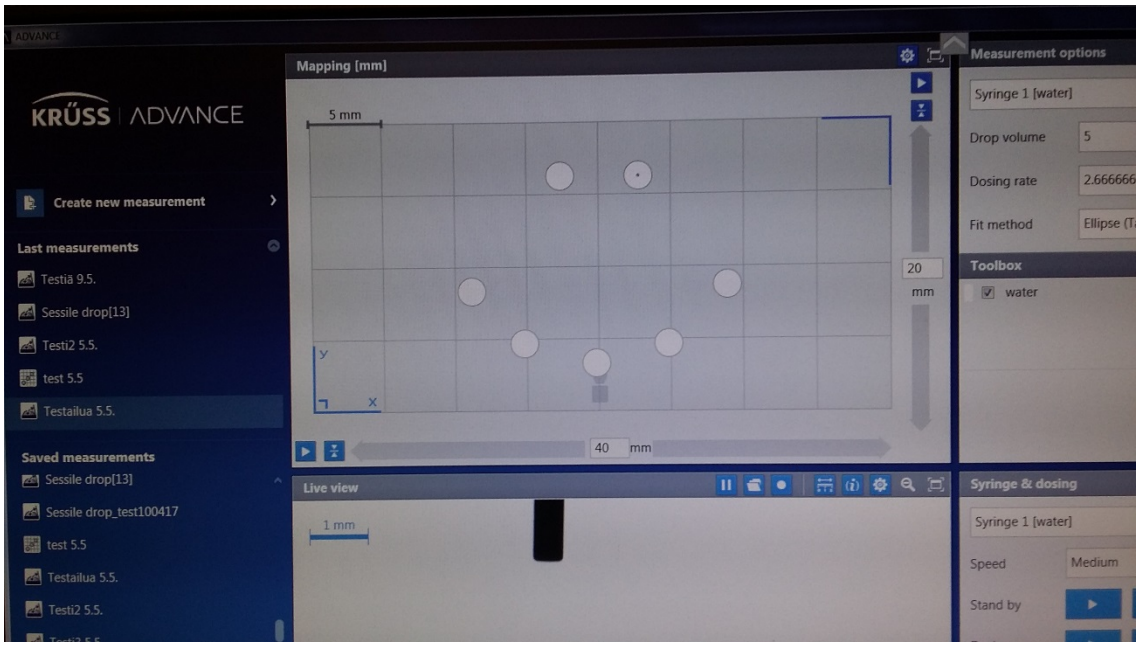

PICTURE 20. Example of sample map

Appendix 2. Measurement table for tilting angle and static contact angle measurements

TABLE 12. Measurements with Krüss DSA100S, part 1/3

			RT					
	Sample name	Code	TILT	DynCA	WCA	EtGlCA	DIMCA	SFE
1	PE1		-		89,5	64,96	51,42	35,04
2	PE2		-		90,57	66,35	51,28	34,53
3	PE3		-		95,02	67,51	53,33	33,02
4	PE4		-		96,03	69,54	53,81	32,6
5	**PE-average**		-		**92,8**	**67,1**	**52,5**	**33,8**
6	PE-UHWM1		-		94,2	69,64	52,16	33,34
7	PE-UHWM2		69		87,23	63,62	51,89	34,27
8	PE-UHWM3		76		84,8	62,4	51,93	34,45
9	PE-UHWM4		71		89,11	61,51	50,33	35,35
10	**PE-UHWM-av.**				**88,8**	**64,3**	**51,6**	**34,4**
11	PP1		69		95,77	76,61	56,34	27,21
12	PP2		54		97,41	79,66	59,04	29,03
13	PP3		54		99,35	80,25	59,64	27,32
14	PP4		-		97,34	80,2	61,63	27,43
15	**PP-average**				**97,5**	**79,2**	**59,2**	**27,7**
16	PTFE1		-		97,6	86,52	81,6	18,53
17	PTFE2		-		103,66	82,26	79,26	19,17
18	PTFE3		-		103,71	87,94	78,81	19,22
19	PTFE4		-		104,06	76,16	83,13	18,04
20	**PTFE-av.**				**102,3**	**83,2**	**80,7**	**18,7**
21	PU1		-		108,6	81,11	54,98	31,24
22	PU2		-		100,2	74,05	49,5	34,52
23	PU3		-		95,41	76,82	50,82	33,7
24	PU4		-		96,64	76,18	44,18	33,55
25	**PU-average**				**100,2**	**77,0**	**49,9**	**33,3**
26	Ref-Al		-				55,75	

Appendix 3. Measurement table for Peltier plate at RT and +15 °C

TABLE 13. Measurements with Krüss DSA100S, part 2/3

+21°C				+15°C			
WCA	EtGlCA	DIMCA	SFE	WCA	EtGlCA	DIMCA	SFE
87,63	67,11	53,56	32,29	76,93	67,02	54,7	32,57
86,69	64,39	53,74	33,35	75,4	64,49	54,75	32,63
83,71	66,16	53,58	33,7	75,59	64,4	53,45	33,24
82,48	70,49	54,54	32,34	76,34	75,04	55,75	30,54
85,1	**67,0**	**53,9**	**32,9**	**76,1**	**67,7**	**54,7**	**32,2**
80,58	67,02	53,67	32,97	77,11	68,26	53,63	32,93
85,21	70,24	52,64	32,64	77,71	65,71	52,3	33,65
84,77	66,74	52,39	33,05	76,78	66,38	52,36	33,69
82,95	66,85	52,51	33,99	77,52	66,82	51,73	34,96
83,4	**67,7**	**52,8**	**33,2**	**77,3**	**66,8**	**52,5**	**33,8**
90,67	76,91	58,33	31,21	92,58	76,72	59,92	30,3
93,15	75,64	57,55	31,32	95,2	73,7	58,64	29,73
92,15	78,76	57,73	30,62	94,4	74,03	58,16	30,41
95,41	76,96	58	29,82	94,82	78,9	59,3	29
92,8	**77,1**	**57,9**	**30,7**	**94,3**	**75,8**	**59,0**	**29,9**
93,77	87,52	79,66	18,53	101,07	79,54	80,75	19,17
99,58	87,06	81,97	17,15	89,17	87,89	81,77	16,99
92,49	87,93	81,51	16,72	91,26	84,09	82,91	18,81
99,93	86,9	80,79	15,73	93,23	87,03	82,49	17,48
96,4	**87,4**	**81,0**	**17,0**	**93,7**	**84,6**	**82,0**	**18,1**
96,87	67,87	57,15	31,65	77,56	71,14	56,53	26,86
86,88	67,2	45,8	37,48	78,19	71,13	47,63	34,6
86,86	70,09	45,62	35,27	81,91	64,43	46,27	36,94
90,79	69,86	52,79	28,59	78,15	73,88	49,77	22,21
90,4	**68,8**	**50,3**	**33,2**	**79,0**	**70,1**	**50,1**	**30,2**
86,56	70,56	59,16	29,35	81,23	69,33	57,32	32,07

Appendix 4. Measurement table for Peltier plate at +10 °C and +5 °C

TABLE 14. Measurements with Krüss DSA100S, part 3/3

+10°C				+5°C			
WCA	EtGlCA	DIMCA	SFE	WCA	EtGlCA	DIMCA	SFE
85,25	65,97	52,49	34,24	80,53	66,43	51,82	34,01
72,72	63,27	54,22	35,42	76,82	65,77	53,57	34,1
63,89	63,3	53,61	38,7	69,95	63,32	52,45	41,09
66,98	68,7	52,41	33,3	71,52	66,1	54,44	34,21
72,2	**65,3**	**53,2**	**35,4**	**74,7**	**65,4**	**53,1**	**35,9**
73,74	65,45	54,08	33,23	71,52	61,65	53,59	33,88
75,93	65,31	51,58	34,03	75,03	64,56	53,94	33,13
72,62	65,12	52,56	39,81	74,48	62,99	52,61	37,02
70,95	65,25	51,99	33,28	72,95	59,65	51,51	39,72
73,3	**65,3**	**52,6**	**35,1**	**73,5**	**62,2**	**52,9**	**35,9**
87,74	75,04	60,56	30,24	85,24	72,56	61,03	28,5
93,83	72,73	59,09	29,87	88,71	72,67	59,58	30,46
90,27	71,92	58,13	30,39	88,6	72,61	59,6	30,89
93,05	74,45	60,72	28,5	90,43	74,75	60,45	28,71
91,2	**73,5**	**59,6**	**29,8**	**88,2**	**73,1**	**60,2**	**29,6**
91,64	77,25	83,44	20,66	92,08	83,41	82,58	19,88
89,61	84,8	81,61	16,64	88,84	84,65	79,2	17,51
92,22	86,11	83,2	17,71	90,06	82,45	80,31	21,59
92,38	87,16	82,12	17,39	91,75	86,6	79,69	18,22
91,5	**83,8**	**82,6**	**18,1**	**90,7**	**84,3**	**80,4**	**19,3**
74,98	70,97	46,59	35,39	64,75	58,62	46,99	33,06
73,23	67,99	46,41	37,02	77,31	65,06	48,74	30,94
71,84	68,06	46,03	37,06	67,21	60,99	47,78	44,91
66,96	64,02	53,59	39,21	67,5	65,57	48,9	41,13
71,8	**67,8**	**48,2**	**37,2**	**69,2**	**62,6**	**48,1**	**37,5**
76,57	70,19	56,93	26,81	71,77	71,48	56,25	32,31